USE OF FOURIER TRANSFORM-INFRARED SPECTROSCOPIC IMAGING AS A TOOL FOR UNDERSTANDING EARLY MOLECULAR EVENTS DRIVING BREAST CANCER PROGRESSION

BY

SARAH ELIZABETH HOLTON

THESIS

Submitted in partial fulfillment of the requirements
for the degree of Master of Science in Bioengineering
in the Graduate College of the
University of Illinois at Urbana-Champaign, 2010

Urbana, Illinois

Adviser:

Professor Rohit Bhargava

ABSTRACT

The presence of an activated stroma surrounding a primary breast tumor is a well-documented phenomenon. Fibroblasts are the cell type responsible for maintaining the stroma, and cancer-associated fibroblasts, characterized by the expression of α-smooth muscle actin (α-SMA) protein, are highly contractile compared with those found in normal tissue, and may aid in tumor progression. Although the fibroblast to myofibroblast phenotypic transition is drastic and involves changes in cell morphology as well as increased expression of proteins, the best marker for myofibroblasts used in both the laboratory and the clinic is α-SMA. Due to the role of the stroma, in general, and the fibroblast in particular, in cancer progression, it is important to study this characteristic cellular transformation *in vitro*. We report a direct comparison between α-SMA expression in primary normal human dermal fibroblasts and molecular spectra obtained through Fourier Transform infrared (FT-IR) spectroscopic imaging. Fibroblasts were stimulated using the growth factor TGFβ1, co-culture with MCF-7 tumorigenic breast epithelial cells, and co-culture with MCF10A normal breast epithelial cells in trans-well co-culture and also three-dimensional cell culture. α-SMA expression was determined using immunofluorescence and the samples were surveyed in a holistic and label-free approach using chemical imaging in two modes: transflection and attenuated total reflectance (ATR) FT-IR. This correlation is also compared with expression of α-SMA and spectra obtained from normal and tumorigenic human breast tissue biopsies.

For my parents, John and Cornelia Holton

ACKNOWLEDGEMENTS

I would first and foremost like to thank my parents, for giving me the inspiration and encouragement to pursue my love of science. Thank you to my adviser, Dr. Rohit Bhargava, for providing the tools, resources, and motivation for this project. Many thanks also to the members of the Chemical Imaging and Structures Laboratory, in particular Dr. Michael Walsh, who trained me in biospectroscopy and provided guidance and support along the way. Many thanks to the Medical Scholars Program for allowing the flexibility to pursue an MD/PhD in Bioengineering. I would also like to thank the SURGE fellowship, which provides funding for students traditionally underrepresented in engineering. This very important program let me explore my options at the University of Illinois (and there are many!). Finally, thank you to my friends for your unwavering support and commiseration.

TABLE OF CONTENTS

CHAPTER 1: INTRODUCTION

Although it is understood that the stromal tissue surrounding an epithelial tumor is chemically changed during cancer progression, the steps of biochemical evolution are not well characterized. Understanding the chemical progression and its time course will lead to a better understanding of disease progression and may eventually lead to novel targeted therapies that will be successful for more patients than current options. The main cell type comprising the stroma, and the one which maintains the balance of collagen production and degradation in the stroma, is the fibroblast. One of the best characterized changes in a cancer-associated stroma is the fibroblast to myofibroblast phenotypic change, distinguished by the expression of α-SMA in the cytoplasm of activated cells. The expression of this cytoskeletal protein results in the stiffening of the tumor microenvironment, which has implications in cancer progression (Goffin, 2006)(Ong, 2009)(Rønnov-Jessen, 1995)(Kong, 2010)(Rozenchan, 2009). This stromal stiffening due to the fibroblast to myofibroblast transition may also play a role in lung fibrosis and wound management (Rønnov-Jessen, 1995).

Normal fibroblasts co-cultured with cancerous epithelial cells undergo the fibroblast to myofibroblast phenotypic change, and characteristically express α-SMA (Rønnov-Jessen, 1995)(Rozenchan, 2009). Similarly, when normal fibroblasts are stimulated with TGF-β1, a growth factor that is known to have multiple roles in tumor growth and the conditioning of the microenvironment (Rønnov-Jessen, 1995), α-SMA is expressed. This expression is measured using immunofluorescence, an antibody-based technique. There are limitations in using antibody-based techniques as they are time-

consuming, costly, and it is difficult to use them to quantify protein expression. Similarly, immunofluorescence only measures the expression of several proteins simultaneously, which is not enough information when considering the cytopathic effects of a multifactorial disease like cancer. A holistic and multiplexed study of the fibroblast to myofibroblast differentiation is needed to fully understand why this is such a conserved phenotype across cancers of multiple tissues.

Fourier transform infrared (FT-IR) spectroscopy has been used to study biochemical changes that occur within cells undergoing disease processes in a label-free manner (Kong, 2010)(Bird, 2008)(Bogomolny, 2008)(Bogomolny, 2007)(Diem, 2004)(Salman, 2004)(Harvey, 2009)(Lasch, 2002)(Baker, 2010)(Lee, 2009). However, this is the first report of a correlation between the expression of a specific protein and its associated spectroscopic signature in two-dimensional and three-dimensional cell culture and human breast tumor biopsies. FT-IR measures the characteristic absorption of energy by chemical bonds present in a sample. A wide variety of biomolecules, including nucleic acids, collagen, glycogen, proteins, and fatty acids, absorb in the mid-infrared range (λ = 2-20 μm), which allows FT-IR to be useful for determining global biochemical changes that occur within a sample. The benefit of using FT-IR over other biological imaging modalities is that it is label-free with the current limitation that the sample must be fixed and dried. Using FT-IR as a holistic first pass approach can yield information about ways in which samples are changing. This can give an indication of which biological assays to perform next.

The purpose of these experiments was to compare the expression of α-SMA protein in primary normal dermal fibroblasts activated with TGFβ1 and also co-culture with MCF-7

tumorigenic breast epithelial cells to chemical spectra obtained through FT-IR imaging. In order to see the effects of a tumorigenic breast epithelium on the surrounding tissue stroma, two co-culture methods were utilized. First, the transwell co-culture allows for two cell types to communicate via soluble growth factors diffused into a shared medium (Rozenchan, 2009). Primary normal human dermal fibroblasts (NDF) were grown on MirrIR slides, which allowed for both FT-IR and immunofluorescence analysis after the experiment. The fibroblasts were co-cultured with tumorigenic breast epithelial cells, MCF-7, nontumorigenic breast epithelial cells, MCF10A, or stimulated with TGFβ1, a growth factor known to induce the fibroblast to myofibroblast phenotypic change. Over time, samples were fixed and half were analyzed using immunofluorescence to detect the presence of α-SMA protein. The other samples were imaged using FT-IR.

Additionally, a three-dimensional cellular co-culture model was developed as an analog of the transwell co-culture. The three-dimensional model consists of cells embedded in a type I collagen hydrogel. The samples were prepared as separate layers, with one cell type (NDF, MCF-7, MCF10A) per layer. This allows for the layers to be stacked in different ways, co-cultured for a determined length of time, and then separated easily with forceps.

There was no observed cell migration within the time course of this experiment, determined by cell type specific expression of cytokeratins for epithelial cells and vimentin for fibroblasts (Data not shown). This model allows for cellular co-culture in a more realistic three-dimensional environment with cell-type specific analysis for future biological assays. For the scope of this experiment, it shows that fibroblast activation can be controlled by diffusion of small molecules from a cancerous epithelium through the stroma. Additionally, the three-dimensional culture model described here uses FT-IR to

study the effects of a cancerous epithelium and an activated stroma on the surrounding tissue microenvironment, which has been demonstrated previously in an engineered skin model (Kong, 2010).

Finally, the expression of α-SMA and spectroscopic signatures of human breast tissue biopsies were compared in order to determine how these experiments translate into a more clinical system. α-SMA expression was measured using immunohistochemistry (IHC). For FT-IR measurements, the tissue samples were placed on a barium fluoride plate and scanned in a transmission mode.

The current limitation of FT-IR imaging is its poor spatial resolution. Although chemical changes can be seen by comparing entire samples, this represents an entire population of cells. If there is clonality in the population, or there are chemical changes as a function of distance from the cancerous source, FT-IR imaging in transmission or transflectance mode may not be sensitive enough for detection using commercial, benchtop systems like the Perkin-Elmer Spotlight used in this work. However, there is a mode of FT-IR imaging known as attenuated total reflectance (ATR) in which a high refractive index material is placed in close proximity to the sample such that the resulting evanescent wave arising from reflection within the high index material is used to interrogate the sample (Sommer, 2001)(Kazarian, 2003). ATR spectroscopy is generally useful for biological experiments because samples do not necessarily need to be dried, as is the case in other FT-IR modes. Since the evanescent wave set up has a limited penetration depth into the sample (0.5 – 5 μm), cells can be grown on substrates normally used for cell culture little spectral contribution. Since the sampled volume is fixed, ATR data are also hypothesized to be less prone to optical distortions which can be a problem with biologically-derived

samples in other reflection modalities (Brown, 2007)(Dumas, 2009). These benefits allow for a direct comparison between biological phenomenon and spectral signatures, making ATR FT-IR spectroscopic imaging a potentially powerful tool in the laboratory. A further advantage of ATR imaging is the increase in effective numerical aperture due to the high index material acting as a solid immersion lens (Ippolito, 2005). Used in conjunction with an IR microscope, this leads directly to a higher spatial resolution than available using transmission or reflection mode sampling (Brown, 2007)(Dumas, 2009).

Here, we sought to further examine the early transformations in fibroblasts in cell culture to elucidate the spectroscopic characteristics of the fibroblast to myofibroblast transition by using the ATR mode of FT-IR. Then, we looked to examine and compare spectral characteristics of the transition in primary adult human dermal fibroblasts using two approaches: first, activation through TGF-β1 stimulation and, second, co-culture with a cancerous breast epithelial line. While the former is important to trace the transition to a molecular event, the latter is likely more reflective of the processes in complex tissue. Spectroscopic measurements were compared to immunofluorescence staining for α-SMA, the best characterized marker for the fibroblast to myofibroblast transition.

CHAPTER 2: BACKGROUND

Section 2.1 Cancer and the Tumor Microenvironment

Although cancer is a disease that has been well-documented throughout history, it was not until the 1970s that a scientific basis for the cause of the disease was proposed. With the discovery of the first oncogene, *src*, and *Rb* soon after, a genetic basis for the initiation of cancer within adult tissues was determined (Mendelsohn, 2008). An oncogene is a gene which when normally expressed, helps regulate cell growth and differentiation. However, when it is mutated or the expression is amplified (through a gain of function mutation or disregulation due to environmental factors), it can give rise to uncontrolled cellular proliferation which can form a tumor. The literature for the next twenty years was devoted to the discovery of novel oncogenes, which led to a greater understanding of the types of genetic mutations that can occur, such as single nucleotide polymorphisms (SNPs). There are now commercially-available kits for detecting common mutations, most notably the BRCA1 gene which is implicated in familial breast cancer (Davies, 1996).

While it is clear that cancer is initiated by the accumulation of genetic mutations, recent evidence suggests that the interplay between cells and their local environment may drive tumor progression or make certain tissues more susceptible for neoplastic growth. In breast cancer, carcinoma arises in the epithelial compartment of the tissue. The epithelium, which comprises the lining of each glandular unit, is then surrounded by a dense connective tissue comprised of collagen and cells that maintain it such as fibroblasts and pericytes. Cells involved in the immune system, such as macrophages, are also found here. This collagen-rich tissue is known as intra-lobular stroma. Surrounding each ductal unit is

more collagen-rich stroma, known as inter-lobular stroma. This distinction is made through the histological section of breast tissue shown in **Figure 2.1**. While mutations in the epithelium initiate tumor progression, the outcome of the tumor may be regulated by the stroma. From now on, this cell-environment interaction will be referred to as stromal-epithelial interactions.

Although most therapeutic efforts to date for treating cancer are targeted towards the epithelium, it has been shown that a cancerous phenotype can be either suppressed or enhanced simply by manipulating the stroma. In 1975, Illmensee et al. showed that when cells from a teratoma were surrounded by an embryonic stroma *in vitro*, the tumor cells became reprogrammed and formed normal tissue in a developing mouse. (Illmensee, 1976). Then, in 1984, Dolberg and Bissell injected the RSV oncovirus into chickens before and after hatching. Although the chickens injected after they had hatched developed tumors, as was expected, the chickens that were injected in the egg developed normally (Dolberg, 1984). There is something about the embryonic microenvironment that can suppress tumor growth and metastasis on a level that is higher than genetics. Some biological phenomena which act to regulate genetics are small factors that control the expression of genes such as microRNAs and growth factors released from neighboring cells, mechanical or fluid forces that may transduce signals into the epithelium, and the body's innate immune response. Similarly, the cancerous phenotype can be promoted simply by treating the stroma. For example, in co-culture models with senescent fibroblasts, epithelial cells were more migratory and had a greater proliferative potential than cells cultured with non-senescent fibroblasts (Barcellos-Hoff, 2005). This suggests that the accumulation of mutations in fibroblasts may lead to a signaling pathway which confers similar genetic

mutations in adjacent epithelial cells, but this is a difficult hypothesis to test. In breast cancer, it has been noted since mammography became prevalent in the clinic as a routine procedure that an increase in mammographic collagen density is correlated with a more aggressive and invasive disease. This has also been demonstrated in mouse models in which the only risk factor is increased levels of collagen in the mammary tissue (Provenzano, 2006). The role of the microenvironment in driving tumor progression is becoming more evident, and it has been suggested that the tumor stroma may be a therapeutic target in the future (Ingber, 2008).

Section 2.2 Fibroblast to Myofibroblast Transition

Many morphologic and physiologic changes occur in the tissue comprising and surrounding a tumor; looking at biopsies under the microscope is still one of the best methods for diagnosing cancer. One characteristic cellular change is the fibroblast to myofibroblast transition. This is a phenotypic change that is characterized in both biological and clinical laboratories by the expression of the protein α-smooth muscle actin (α-SMA). α-SMA is an actin isoform, and it integrates with the cell's stress fibers, which act like tent poles to help stabilize the cell on its surface. These fibers with incorporated α-SMA are shown in **Figure 2.2**. Fibroblasts which express α-SMA also display other characteristics of cells found in muscle. They are more contractile and tend to lengthen along axes that give them traction. In three-dimensional culture, activated fibroblasts grown in collagen will create so much tension that the gel collapses (McDaniel, 2006). These cells are found in the stroma immediately surrounding tumors, but not elsewhere in the stroma (unless the disease has progressed to a highly invasive stage). The physical and

chemical changes that occur in this 'activated stroma' may aid the tumor cell in intravasation (entering the blood circulation) and further dissemination into distal tissues.

For studying this process *in vitro*, transforming growth factor- β1 (TGFβ1) is used in order to differentiate fibroblasts into a myofibroblast state (Rønnov-Jessen, 1996) (Rønnov-Jessen, 1995). TGFβ1 activates the Smad pathway, which is implicated in many diseases including cancer and fibrosis (Moses, 2010). Activation of Smad signaling via TGFβ1 has many downstream effects, including activation of Ras, Erk, and PI3K, and inhibition of mTor through activation of Akt (Moses, 2010). This pathway is especially important in breast cancer, because breast epithelial cells are highly sensitive to stromal TGFβ1. In normal tissue, TGFβ1 acts to inhibit proliferation and morphogenesis in the dormant breast via autocrine (signals within the same cell) and paracrine (local signals between cells) signaling. It does this by mediating the cell response to the ovarian hormones, estrogen and progesterone. When this system becomes deregulated, the results can be disastrous. The unnecessary remodeling of mammary epithelium or stroma in response to uncontrolled hormone stimulation gives rise to carcinomas, which can progress to metastatic disease. It is evident that this pathway should be understood on multiple levels as it fits into stromal-epithelial interactions for the development of therapeutic interventions.

Section 2.3 Fourier Transform Infrared (FT-IR) Spectroscopic Imaging

Fourier transform infrared (FT-IR) spectroscopic imaging is a label-free technique that uses light absorption in order to quantify the relative amounts and distributions of chemical bonds present within a sample (Bird, 2008). Infrared radiation is outside the

visible spectrum, with wavelengths between 0.7 and 300 μm. These wavelengths can be further broken down into the near infrared (NIR), 0.7 to 2 μm, the mid infrared (MIR), 2 to 50 μm, and the far infrared (FIR), 50 – 1000 μm (ISO 20473 scheme). The delineations between the three categories are not steadfast, and to some extent rely on the ranges of wavelengths that different IR detectors can sense (Miller, 2004). Using the near, mid, and far infrared regions of the spectrum can also yield information about different types of chemical species.

Vibrational spectroscopy is based on the phenomenon that chemical bonds will absorb energy and vibrate at different characteristic frequencies. Therefore, by directing a known amount of energy into a sample and detecting the radiation on the other side, the chemical species present within the sample can be determined. Infrared spectroscopy is used often in the analytical chemistry field, as a quality control measure. However, in the past twenty years, this technology has also been applied to biological samples, primarily human cells and tissues for the study of disease processes through chemical changes (Baker, 2010) (Bird, 2008) (Bogomolny, 2007) (Bogomolny, 2008). In cell culture, FT-IR spectroscopy has been used in order to detect chemical changes in keratinocytes (skin cells) induced by the cell's growth substrate (Meade, 2007). It has also been used to look at viral progression (Bogomolny, 2008) and cellular transfection with the human oncogene H-ras (Ramesh, 2001). In human tissues, FT-IR is used to differentiate between different cell types for automated histological staining (Fernandez, 2005). This allows for the information which comes from multiplexing of histological stains to be applied in a label-free manner to unstained human tissue. Finally, chemical imaging has been used to look at three-dimensional cell culture models of human skin cancer in order to determine the

distance from a tumor that it can be detected chemically (Kong, 2010). This could be used for intra-operative surgical probes that help to define tumor margins without the need for followup histology. FT-IR is a very powerful tool for studying biological phenomena at the level of basic science as well as in the clinic.

A theoretical schematic of the PerkinElmer Spotlight instrument in transflection mode used for this work is shown in **Figure 2.3**. It is a commercial system and therefore the true schematic is proprietary. The Spotlight is an upright benchtop unit consisting of a microscope with attached liquid nitrogen dewar and motorized x-y-z stage with controller and a separate unit that houses the infrared source and the interferometer. The microscope allows for infrared mapping to be done, which is very useful when working with heterogeneous samples such as tissue mounts. First, a visible image is collected across the entire sample. Then, regions of interest are labeled and the stage coordinates are saved such that multiple regions can be scanned consecutively. In order to scan in transflection mode, as was done in these experiments, radiation in the mid-IR is generated with a heated filament source, is passed through a Michelson interferometer, and directed through the objective and into the sample. Then, the radiation is reflected from the IR-reflective coating on the sample substrate, passes back through the objective and into a mercury cadmium telluride (MCT) IR detector. This detector needs to be cooled by liquid nitrogen, supplied by the dewar that sits on top of the instrument, in order to be sensitive to small chemical changes. A computer interface is used in order to control the stage and to view the visible image. There are various parameters that can be set, including spectral resolution, number of co-adds, interferometer speed, and pixel size. The default pixel size for the benchtop system in transflection mode is 6.25 x 6.25 μm, which is sufficient for looking at average

chemical changes across a sample in cell biology experiments (Bogomolny, 2007) or in order to classify cell types in tumor biopsies (Fernandez, 2005). The other parameters can change the signal to noise ratio and data quality, and they should be tuned for the type of sample being imaged.

Another mode used in FT-IR spectroscopy is attenuated total reflectance (ATR). This mode places a crystal made of a material with high refractive index directly in contact with the sample. The area that is scanned is limited (by the size of the crystal, usually 500 μm x 500 μm to 1 mm x 1 mm), but the resulting image has a greater spatial resolution. The pixel size is reduced from 6.25 μm x 6.25 μm to 1.56 μm x 1.56 μm, due to the germanium ATR element used acting as a solid immersion lens (refractive index = 4.0). This mode is also less prone to optical distortions as the sampling length scale (1-2 μm) is typically smaller than the wavelength of light. A schematic of an ATR setup is shown in **Figure 2.4**. However, in this work we used a single-bounce ATR element in order to preserve spatial fidelity.

The resulting dataset is three-dimensional. An image is formed and each pixel represents the chemical spectrum in that area of the sample. A characteristic FT-IR spectrum is shown in **Figure 2.5** Using this data, images can be formed for each peak and this will display the distribution and relative amount of that chemical bond present in the sample as a color coded map. An example of this is shown in **Figure 2.6**. The peak displayed is 2932 cm^{-1}, which corresponds to the asymmetric vibrational mode of CH_2 and CH_3 stretching. This mode corresponds with phospholipids, fatty acids, and triglycerides, and can be used as a marker of metabolism (Kong, 2010) (Harvey, 2009). FT-IR imaging can be used to display the relative quantity and distribution of a number of chemical bonds

present within the same sample. This makes it a very beneficial tool for studying biological phenomena.

Section 2.4 Figures

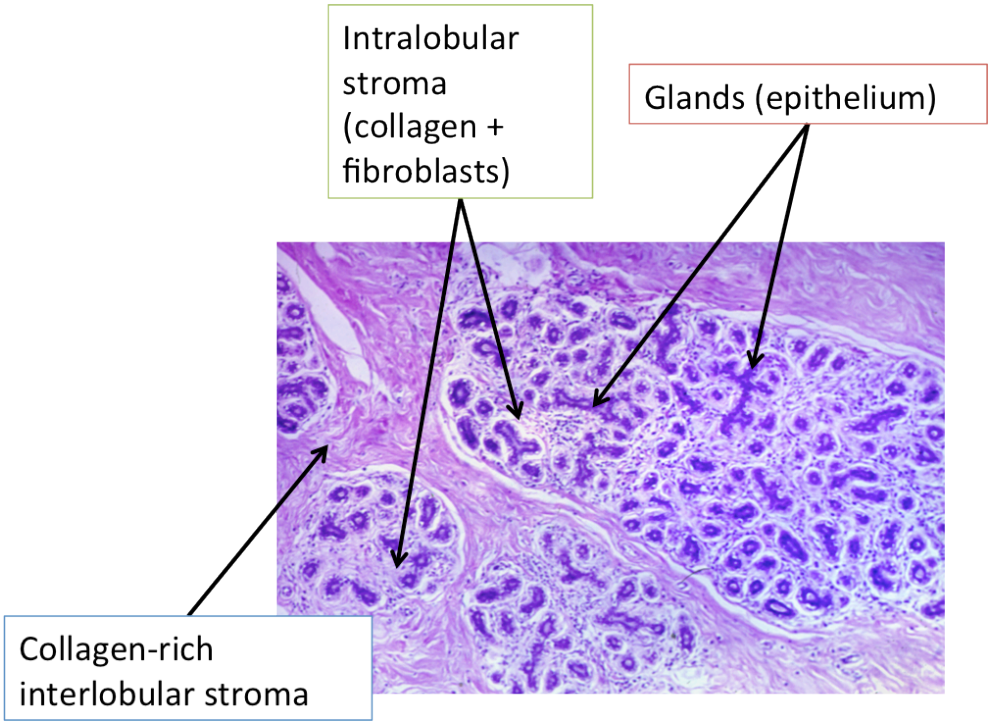

Figure 2.1: Hematoxylin and eosin stained breast tissue section (Anatomy/Histology class, Dr. Hanne Jensen, UC-Davis)

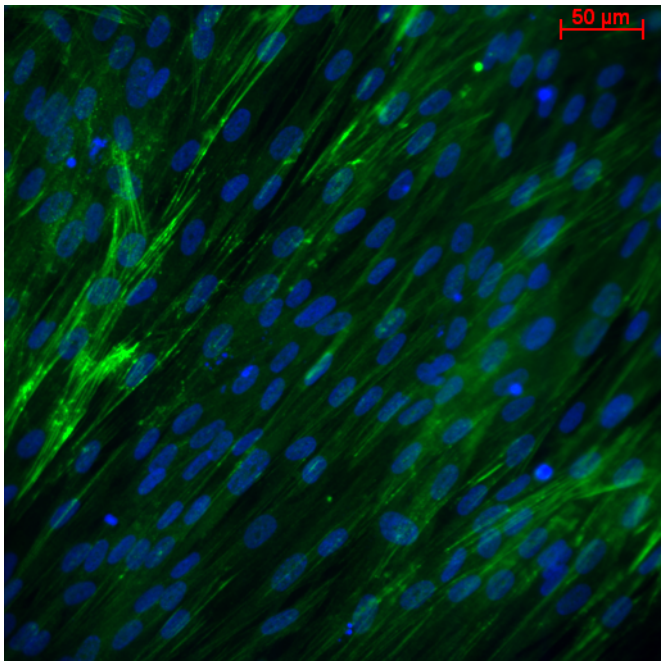

Figure 2.2: α-SMA fibers (labeled with FITC) in lung fibroblasts activated with TGFβ1

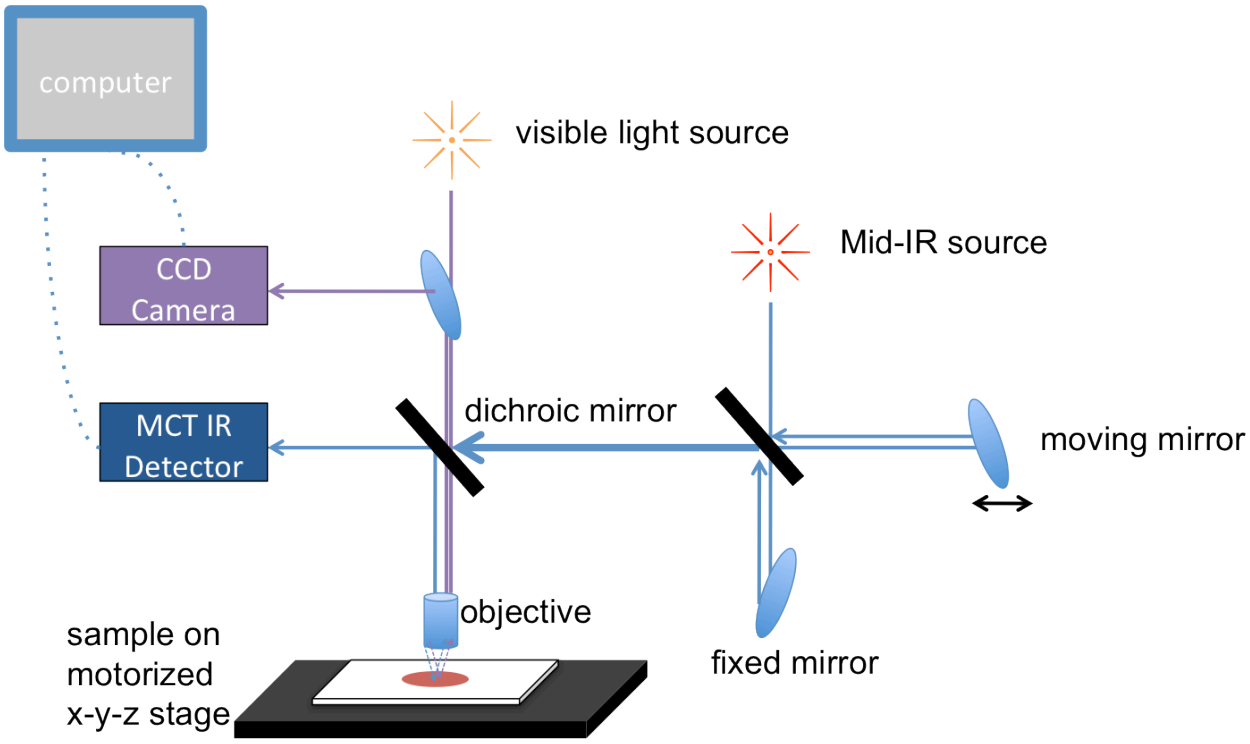

Figure 2.3: Schematic of Spotlight FT-IR Imaging Instrument

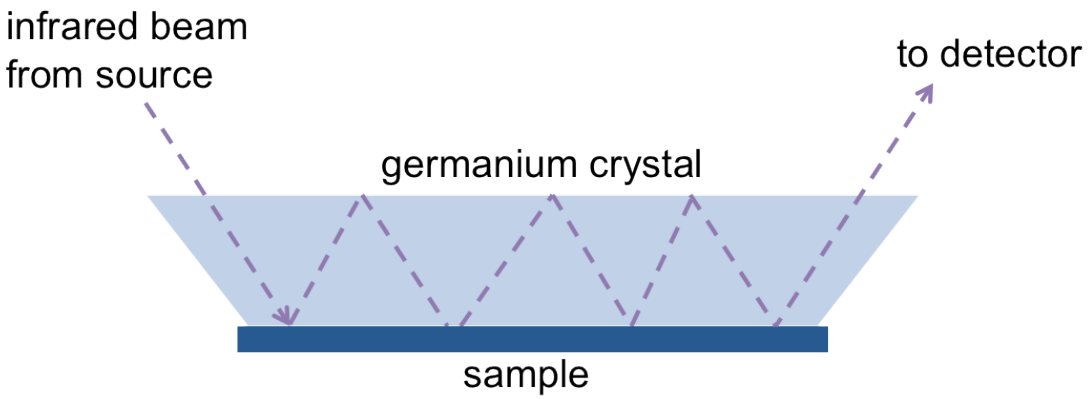

Figure 2.4: ATR FT-IR spectroscopy schematic

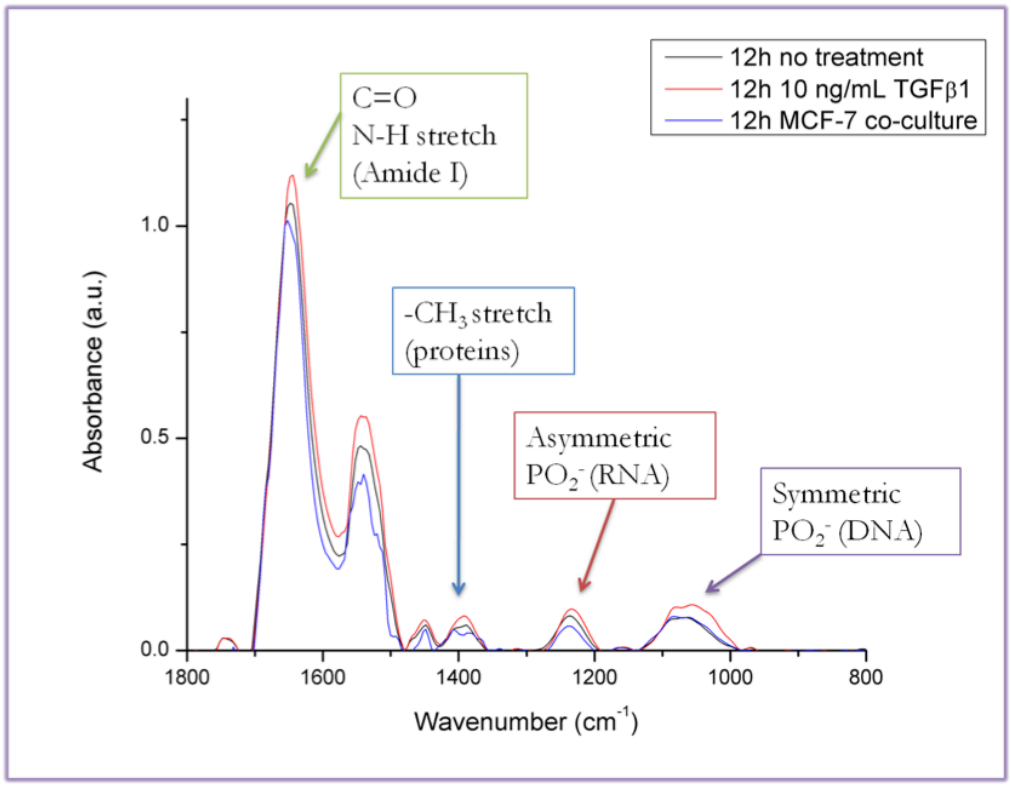

Figure 2.5: Sample IR absorption spectrum with labeled peaks corresponding to common biological quantities

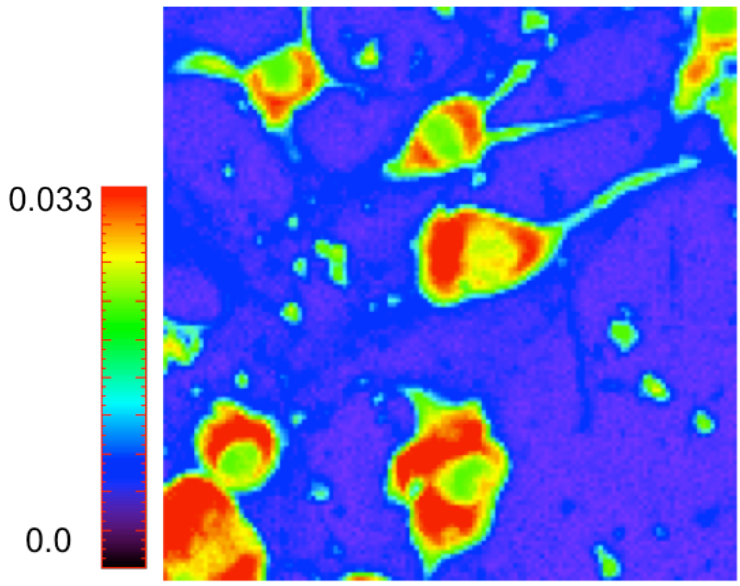

Figure 2.6: IR absorption image of dermal fibroblasts, plotted using the peak intensity of the asymmetric stretching vibrational mode at 2932 cm^{-1}

CHAPTER 3: METHODOLOGY

Section 3.1 Monolayer Cell Culture

The fibroblasts used in this set of experiments were chosen because they are a primary cell line, which are more chemically similar to those in human tissue. They do not endogenously express α-SMA (Sorrell, 2004), but can be induced into the myofibroblast phenotype upon stimulation with TGFβ1 (Rønnov-Jessen, 1995). Also, they are quite large when grown in monolayer culture (approximately 30-50 μm in diameter), and have a large, distinct nucleus (**Figure 3.1**). This is very beneficial for the IR spectroscopic studies because each cell is composed of multiple pixels, which allows for better separation of chemical spectra between samples. Furthermore, the fibroblasts grew in three-dimensional culture for as long as one week without losing morphology or phenotype.

Normal adult primary dermal fibroblasts (NHDF, Lonza, #CC-2511) were maintained in Fibroblast Basal Medium supplemented with 0.1% hFGF-B, 0.1% Insulin, 0.1% gentamicin/amphotericin-B, and 2% FBS (FGM-2 Fibroblast Growth Medium-2 Bullet Kit, Lonza, #CC3132). They were used at passage 8-10 to avoid problems associated with senescence in primary cell lines. The fibroblasts were subcultured according to protocols detailed on the Lonza website, and their ReagentPack (Trypsin/EDTA, Trypsin Neutralizing Solution, HEPES Buffered Saline Solution, #CC-5034) was used exclusively with this cell type. For serum-free medium, the media was prepared the same way except FBS was omitted.

The cell line used to give the cancerous signature in this work was the MCF-7 cell line developed at the Michigan Cancer Foundation (Sadlonova, 2009). It was derived from a

woman with metastatic breast cancer and isolated from a pleural effusion. Although the cells were isolated from a metastatic tumor, MCF-7 have a less cancerous phenotype *in vitro* than some other breast tumor-derived cells such as the MDA-MB-231 line (Sadlonova, 2009). Most notably, the MCF-7 cell line is not highly migratory in two- or three-dimensional culture when assessed using the Boyden chamber assay (Debnath, 2005). MCF-7 cells are estrogen receptor and progesterone receptor positive (ER+/PR+) but do not overexpress Her2/neu protein. They are a luminal epithelial cell (Debnath & Brugge, 2005).

Tumorigenic breast epithelial cells, MCF-7 (ATCC), were maintained in Dulbecco's Modified Eagles Essential Medium (Invitrogen) supplemented with 10% FBS (Sigma) and 1% PenStrep (Sigma). They were subcultured by detaching the cells from the flask with 0.5% trypsin-EDTA (Sigma) for 3 minutes at 37˚C, rescuing in complete growth medium, centrifuging at 1000rpm for 3 minutes, and then resuspending in complete growth medium. MCF-7 cells were subcultured every 3 days at 70% confluency.

Finally, the cell line used to represent the normal breast epithelium is the MCF10A cell line, also developed at the Michigan Cancer Foundation from a patient with fibrocystic disease (Debnath, 2003). MCF10A are not tumorigenic, but they are aneuploid (48, XX +8, +16, -3p, +6p, +9p). They also have characteristics of luminal epithelial cells (Debnath, 2003). Most importantly, they will form polarized, growth-arrested acini when grown for 12-16 days in Matrigel overlay culture. These acini are composed of a single layer of epithelial cells surrounding a central, hollow luminal structure (**Figure 3.4**). The acini behave like normal mammary epithelial tissue, which is why they were chosen as the normal epithelium for these experiments.

Nontumorigenic breast epithelial cells, MCF-10A (a gift from the Muthuswamy lab at Cold Spring Harbor Laboratory and Dr. Supriya Prasanth at UIUC) were maintained in monolayer culture with supplemented medium (DMEM/F12 containing 5% Horse Serum, 20 ng/mL EGF, 0.5 μg/mL Hydrocortisone, 100 ng/mL cholera toxin, 10 μg/mL Insulin, and 1% Pen/Strep) and grown in a 5% CO_2 humidified incubator. They were passaged regularly and maintained according to strict protocol (Debnath, 2003) so that the cells maintained a normal phenotype.

Section 3.2 Transwell Co-culture

Transwell co-culture models are commonly used in order to culture two cell types together without the cells coming into physical contact with one another. There is a membrane in between the cells so they are able to communicate via the free diffusion of soluble growth factors into their shared medium. **Figure 3.5** shows the setup of the transwell co-culture used in this experiment. In order to provide a direct comparison between α-SMA expression visualized using immunofluorescence and FT-IR imaging, a special setup was required. Immunofluorescence imaging requires the sample to be prepared on a glass substrate, because tissue culture plastic can cause aberrations in light transmission. FT-IR requires either an IR-transmissive substrate such as barium fluoride or calcium fluoride or an IR-reflective coating on top of a typical glass slide. This is because glass has a very strong chemical signature in the mid-IR region (Meade, 2007). For this set of experiments, measurements were done in the reflection mode in order to reduce costs associated with using barium or calcium fluoride plates. In order to keep the samples completely consistent between immunofluorescence and FT-IR measurements, NDF were

grown on MirrIR IR-reflective coated glass slides. There did not appear to be any substrate effects on the cells as confirmed by morphology and lack of α-SMA expression at the 0h timepoint.

NDF were grown on pieces of sterilized MirrIR (Kevley Technologies, Chesterland, OH, USA) slides in 12-well plates for 24 hours in complete growth medium, after which they were switched to a serum-free medium for 48 hours in order to halt growth. Simultaneously, MCF10A and MCF-7 were grown on 0.1μm transwell inserts (Corning Incorporated, Corning, NY, USA) for 24 hours in complete growth medium and then switched to serum-free DMEM for 48 hours before co-culture. The 'zero hour' timepoint is defined after 48 hours of culture in serum-free medium. At this time, four samples were fixed in 4% paraformaldehyde. The remaining samples were co-cultured with either MCF-7 or MCF10A. One third of the samples were treated with 1.5 ng/mL TGF-β1 in serum-free medium as a positive control. This concentration is known to induce α-SMA expression in fibroblasts over this time period. Samples were fixed in 4% paraformaldehyde after 6, 12, and 24 hours. The experiments were performed in duplicate with two samples at each timepoint and condition being prepared for immunofluorescence and two samples prepared for FT-IR imaging. The experiment was independently repeated to show reproducibility in both α-SMA expression and IR spectra.

Table 3.1: List of Samples for 2D Co-culture Experiment

Timepoints	Immunofluorescence	FT-IR
0 h	2 no co-culture	2 no co-culture
6 h	2 TGFβ1 2 MCF-7 2 MCF10A	2 TGFβ1 2 MCF-7 2 MCF10A
12 h	2 TGFβ1 2 MCF-7 2 MCF10A	2 TGFβ1 2 MCF-7 2 MCF10A
24 h	2 TGFβ1 2 MCF-7 2 MCF10A	2 TGFβ1 2 MCF-7 2 MCF10A

Section 3.3 Three-dimensional Cell Culture

Three-dimensional cell culture traditionally consists of living cells (one or more cell types) embedded, encapsulated, or suspended within a substrate. The substrate can be a synthetic or biologically derived polymer. In this experiment, the three cell types were suspended in a type I collagen hydrogel. Type I collagen was chosen because it can polymerize under various conditions, giving tunable material properties. Its polymerization is well-characterized, which allows for samples to be made reproducibly in large quantities (Trier, 2009). Furthermore, it is the predominant structural component of the mammary stroma. It has been shown in the literature that collagen density in the mammary stroma has some correlation with outcome in breast cancer patients (Provenzano, 2006). Although these results are intriguing, the collagen density was kept consistent for these experiments, because the cell-cell interaction was the predominant area of focus.

The model used in this work was developed as a three-dimensional analog of the transwell co-culture model in order to study the effects of a cancerous epithelium on normal fibroblasts embedded in a more lifelike environment. It has been shown that cells grown in three-dimensional culture express different receptors on their surfaces when compared with the same cells grown in monolayer culture. Because the fibroblast to myofibroblast phenotypic change is likely driven by the diffusion of growth factors and cytokines through the matrix, it is likely that the expression of these receptors on the surface plays an important role in this phenomenon. Furthermore, FT-IR can be used to visualize the distribution of chemical changes within a sample, and collagen peaks are very distinctive in the chemical spectrum in the mid-IR (**Figure 3.6**). Although collagen density and changes in relation to the fibroblasts was not studied using immunofluorescence, FT-IR is a label-free technique by which these changes can be assessed.

The model itself is layered, shown in **Figure 3.7**. The layers are achieved by sequentially gelling the pre-polymerized collagen that has been mixed with a specific cell type. For example, the gel layer containing fibroblasts is allowed to polymerize first at 37˚C for 1 hour before the next pre-polymer solution is pipetted on top. By preparing the samples in this way, a natural interface is formed between the layers so that they can be physically separated using forceps for further analysis after co-culture. There is no physical barrier separating the two layers. However, early tests were done in order to see whether or not cells migrated through the matrix over a time course of 108 hours. Briefly, a multilayered three-dimensional co-culture model was prepared with fibroblasts (NDF) and epithelial cells (MCF-7) in separate layers. This was prepared in multiple configurations (epithelial cells in top layer, fibroblasts in bottom layer, and vice-versa). Over time, samples

were fixed and stained for cell-specific antigens such as cytokeratins for epithelial cells and vimentin for fibroblasts. There was no cell migration between the layers over the course of the experiment. This is important for cell type-specific analyses in the future, such as genetic and transcriptomic experiments. Because each cell population remains in its individual gel layer, once the layers are separated the cells can be digested for DNA or RNA extraction without the cells having to be separated using bead pull-down assays. Finally, the layered model can be used for co-culturing cells in multiple configurations in order to see how chemical signatures can be propagated through tissue from one cell type to another.

Cells (primary NDF, MCF-7, and MCF10A) were maintained as previously described in two-dimensional culture before being suspended in collagen hydrogels (Type I derived from rat tail, BD Biosciences). All reagents were kept on ice before plating because collagen solution will gel slightly at room temperature. In a conical tube on ice, collagen stock solution was diluted to 2 mg/mL with sterile 10X PBS and mixed with a pipette tip. Cells were trypsinized, centrifuged at 1000 rpm for 3minutes, and resuspended in growth medium. After counting, cells were suspended in the collagen solution at a cell density of 420 cells/mL for NDF and $1.9x10^4$ cells/mL for MCF10A and MCF-7. A much lower cell density of fibroblasts was used compared with epithelial cells because of the tendency of fibroblasts to collapse the hydrogel at high cell density and after activation. Finally, 1N NaOH was added at 0.023 mL per 1mL of collagen stock solution in order to neutralize the acetic acid and allow the collagen to gel. To prepare samples, 200 μL of collagen and cell suspension was added to each well of a 48-well tissue culture plate. The plates were left at 4˚C for 90 minutes in order to slow down the polymerization of collagen to provide a more

uniform fiber orientation and width (Trier, 2009). The samples were then placed in a humidified incubator at 37˚C for 30 minutes to polymerize the collagen with cells embedded inside. After the samples had gelled, fresh warm cell-specific growth medium was added. The cells were allowed to grow for 24 hours before being changed to serum-free medium in order to avoid any confounding effects of growth factors present in FBS or horse serum. After 48 hours in serum-free medium, the co-culture layers were stacked together and 1.5 ng/mL TGFβ1 (Transforming Growth Factor-β1 from human platelets, ≥ 97%, Sigma, #T1654) in serum-free medium was added to some fibroblast samples as a positive control. Fresh serum-free medium was added to the co-cultured samples. The 0h no co-culture samples were fixed in 4% paraformaldehyde and left at 4˚C. After 6, 12, and 24 hours of co-culture, the fibroblast layer was fixed in 4% paraformaldehyde overnight before processing for immunofluorescence or for FT-IR imaging.

Section 3.4 Sample Preparation, Transwell Co-culture

In order to directly compare immunofluorescence to spectroscopic imaging results, after the samples were co-cultured they were prepared in exactly the same way. After fixation, the MirrIR slides were rinsed 3 times with 1X PBS and then covered in 0.10M glycine for 10 minutes to neutralize the paraformaldehyde. The samples were rinsed 3 times with 1X PBS. After this, the samples were divided: for each timepoint, 2 samples were prepared for FT-IR imaging and 2 were prepared for immunofluorescence staining. The samples for FT-IR imaging were rinsed with deionized water and left to dry before imaging. Because it has been suggested that the level of hydration of the sample can affect the recorded absorption spectrum (most notably, the 1080 cm^{-1} band associated with the

asymmetric stretching of the phosphate backbone of nucleic acids), all of the samples were fully dried before imaging.

Section 3.5 Immunofluoresence

After fixation in 4% paraformaldehyde, all samples were washed with PBS and quenched with 0.15 M glycine for ten minutes. After three washes in PBS, half of the samples were subsequently prepared for FT-IR imaging while the other half were processed for analysis using immunofluorescence. The samples for immunofluorescence imaging were permeabilized with 0.2% Triton-X-100 for fifteen minutes. They were washed and then blocked in 1% BSA in PBS/T (phosphate buffered saline containing Tween-20) for 90 minutes. After the blocking step, the samples were washed with PBS/T and incubated with primary antibody (Mouse anti-human α-SMA, Dako, 1:100 dilution in 1% BSA in PBS/T) overnight at 4˚C. The samples were washed again and incubated with secondary antibody (Goat anti-mouse IgG-FITC conjugated, abcam, 1:80 dilution in 1% BSA in PBS/T). The samples were mounted with UltraCruz Mounting Medium for Fluorescence with DAPI (Santa Cruz Biotechnology, Cat # sc-24941) and imaged using a Zeiss Axiovert 200M fluorescence microscope. For the IR samples at 0h and 24h timepoints, this immunofluorescence protocol was repeated after spectroscopic imaging to localize α-SMA stress fibers.

Section 3.6 Immunohistochemistry: Tissue Biopsies

A tissue microarray containing 96 cores from 48 patients was obtained from Biomax (US Biomax, Inc., #BRC961). It was mounted on barium fluoride for FT-IR imaging and then

an adjacent section was cut onto glass for immunohistochemical (IHC) staining of clinically relevant stains, including α-SMA, and routine hematoxylin and eosin (H&E) staining for examining morphology (performed by the University of Illinois at Chicago Medical Center).

Section 3.7 Sample Preparation: 3D Co-culture

After fixation in 4% paraformaldehyde for at least 12 hours, samples were paraffin embedded. First, the paraformaldehyde was gently aspirated from the samples and then the gels were dehydrated by serial ethanol dehydration.

Table 3.2: Procedure for paraffin embedding 3D samples

Reagent	Time
50% Ethanol	1 X 45 min
70% Ethanol	1 x 45 min
80% Ethanol	1 x 45 min
95% Ethanol	1 x 45 min
100% Ethanol	3 x 45 min
xylenes	3 x 45 min
paraffin at 58˚C	3 x 1 hour

The samples were put in 50%, 70%, 80%, and 95% ethanol for 45 minutes each followed by three 45 minute washes in 100% ethanol. The samples were then soaked in xylenes for three 45 minute periods. Finally, the samples were placed in paraffin in a 58˚C oven for three 1 hour periods and then left overnight in paraffin. The samples were mounted in paraffin blocks and sectioned at 5 μm onto MirrIR slides for FT-IR imaging and histological analysis. Samples were gently deparaffinized in hexanes for 24 hours before imaging.

Section 3.8 FT-IR Imaging

FT-IR imaging was conducted using a Perkin Elmer Spotlight Spectrum-400 imaging system. For all cellular samples, both confluent and sparse regions of the sample were imaged in a transflection mode from 4000 cm^{-1} to 750 cm^{-1} at a resolution of 8 cm^{-1} with 32 co-adds, an interferometer speed of 1.0 cm/s and a pixel size of 6.25 x 6.25 μm. A background was collected on the MirrIR slide from 4000 cm^{-1} to 750 cm^{-1} at a resolution of 8 cm^{-1}, with 120 co-adds, an interferometer speed of 1.0 cm/s, and a pixel size of 6.25 x 6.25 μm. Atmospheric correction was performed on the Spotlight instrument, and the files were exported into the ENVI-IDL program. Images were baseline corrected and thresholded at 0.015 a.u. for the band at 1656 cm^{-1} (Amide I). To test for changes in average spectra across each region collected, ROIs were drawn to represent each quadrant of the sample and the average absorbances were calculated. After comparison, it was determined that the only differences across the sample were in the -OH region (3750-3000 cm^{-1}) and therefore these differences were discarded (**Figure 3.8**). Then, an average absorbance was calculated for the cells from confluent regions and these spectra were exported into Excel. The spectra were normalized to Amide I in order to account for variances in cell density. Data were plotted using Origin Software.

For tissue microarray data, a background was collected on the substrate from 4000 to 750 cm^{-1} at a resolution of 4 cm^{-1} with 120 co-adds and 2.2 cm/s mirror speed. Sample data was collected from 4000 to 750 cm^{-1} at 4 cm^{-1} resolution with 2 co-adds and a mirror speed of 2.2 cm/s. A pixel size of 6.25 x 6.25 μm was used. Atmospheric correction was performed on the Spotlight, data was imported into ENVI-IDL and band thresholded at 0.03 a.u. for 1656 cm^{-1} (Amide I). In order to determine spectra of fibroblasts and

myofibroblasts in human tissue, ROIs were drawn corresponding to IHC stains for vimentin (fibroblast) and α-SMA (myofibroblast). Data were plotted using Origin software.

In the attenuated total reflectance (ATR) mode using a Ge lens, the spatial resolution is increased. Each pixel is decreased in size from 6.25 μm in transmission/transflection to 1.56 μm in ATR. 300 x 300 μm regions of the 0h samples and all samples at the 24h timepoint were imaged with the ATR FT-IR configuration at the same spot as transflection measurements for a direct comparison (32 co-adds, 8 cm^{-1} spectral resolution, 1.56 μm pixel size). Prior to imaging, samples were washed with deionized water to remove PBS and then dried.

Section 3.9 Data Analysis

Atmospheric correction and ATR correction were performed using the Spectrum IMAGE program associated with the Spotlight. Files were imported into ENVI-IDL and baseline corrected. MNF transform was used to minimize noise in the ATR FT-IR images. For transflection measurements, peak height at 1656 cm^{-1} (Amide I vibrational mode) was used to segment pixels with an absorbance greater than 0.015 to ensure that only cells were being counted in the measurement. In ATR measurements, the nucleus and cytoplasm could be distinguished. Several hundred "nucleus" pixels and "cytoplasm" pixels were marked as separate regions of interest (ROIs) and average spectra were obtained. Spectra were normalized to 1656 cm^{-1} (Amide I) band in order to account for variability in cell density.

Section 3.10 Figures

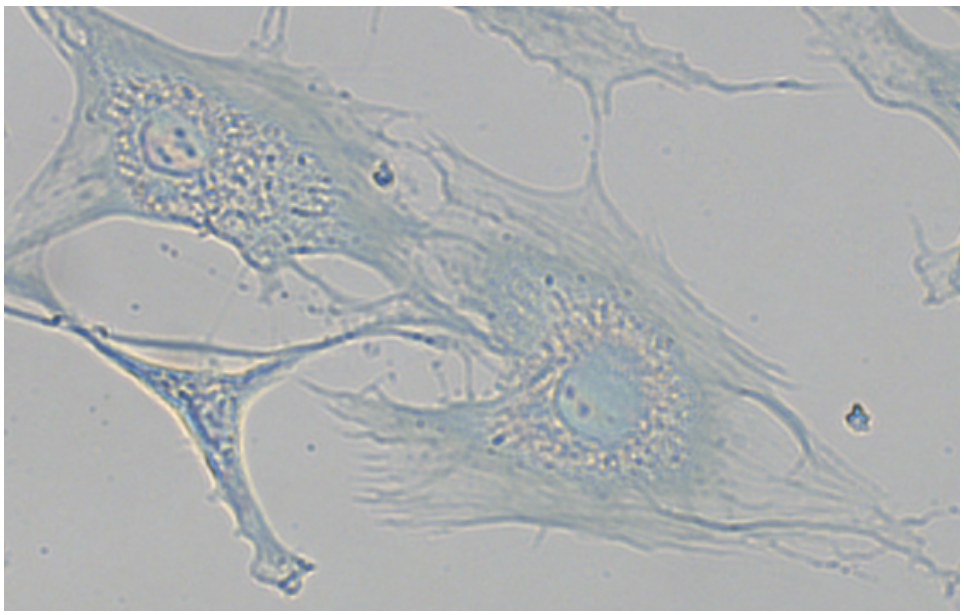

Figure 3.1: Normal Human Dermal Fibroblasts, 40x

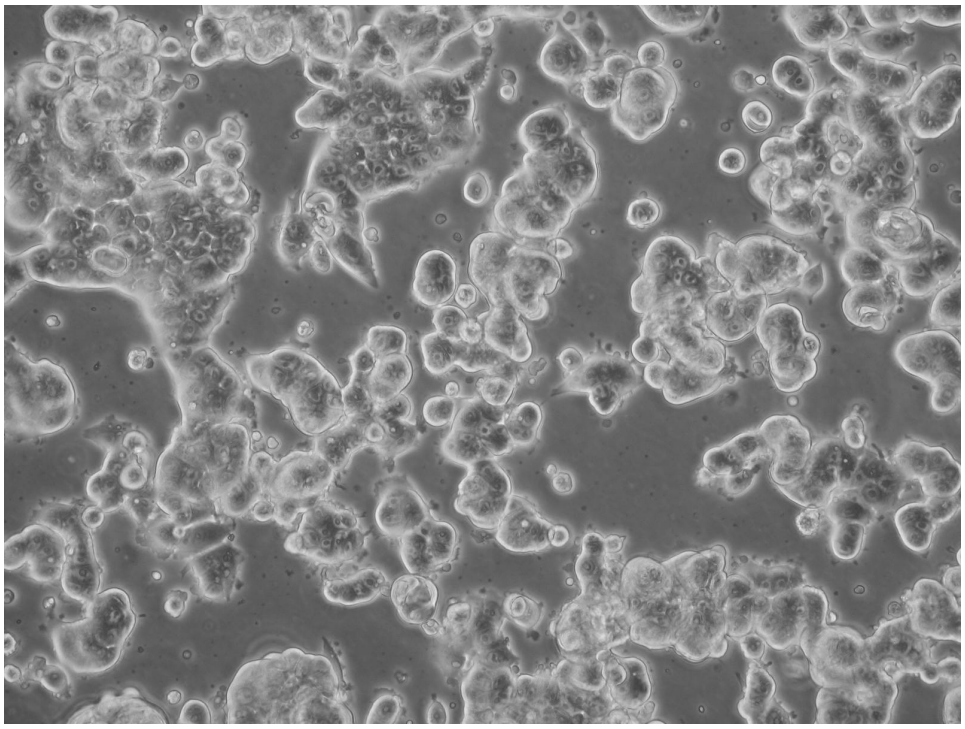

Figure 3.2: MCF-7 monolayer at 20x (Source: Lawrence Berkeley National Laboratory)

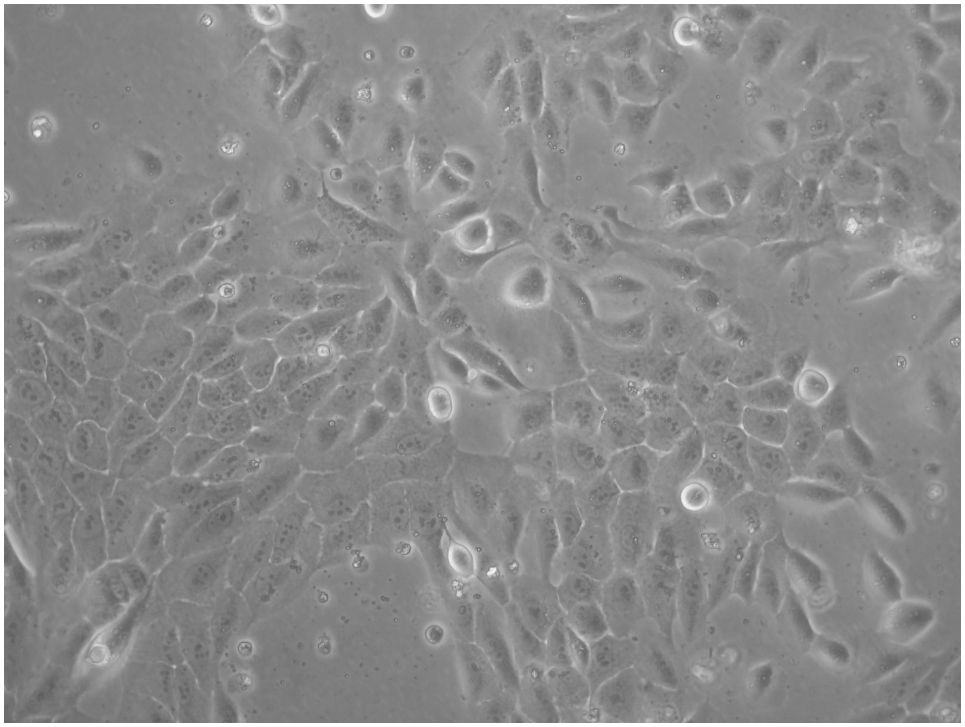

Figure 3.3: MCF10A monolayer at 20x (Source: Lawrence Berkeley National Laboratory)

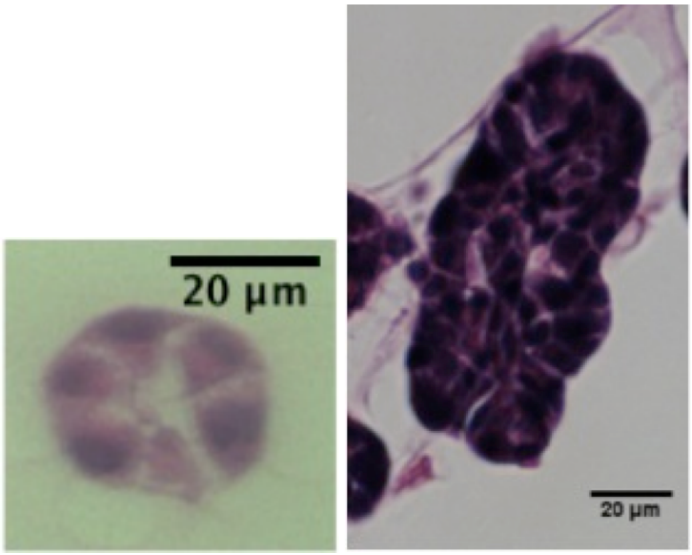

Figure 3.4: Normal (left) and hyperplastic (right) MCF10A Acini (H&E stain) observed in our experiments

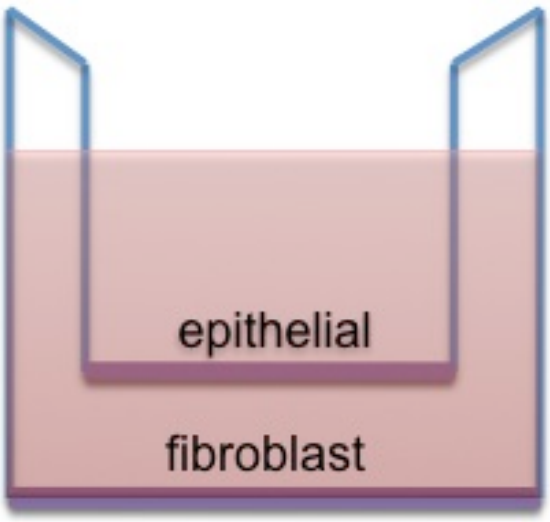

Figure 3.5: Schematic of Transwell Co-culture

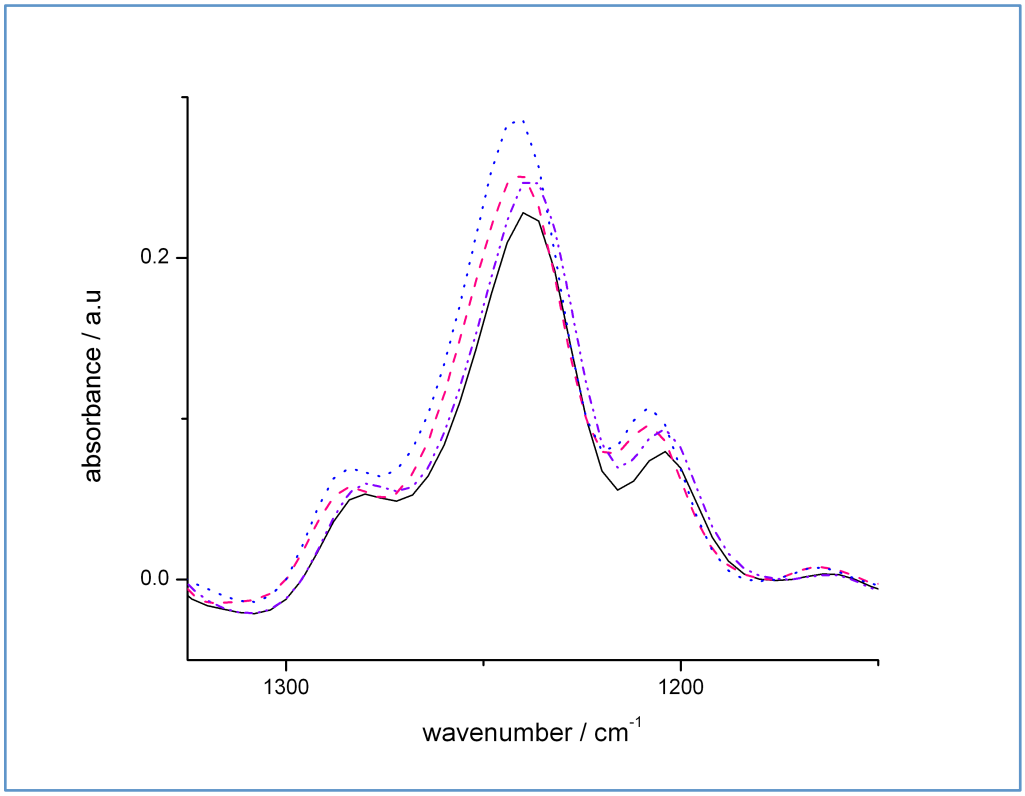

Figure 3.6: Collagen spectra in three-dimensional cell culture

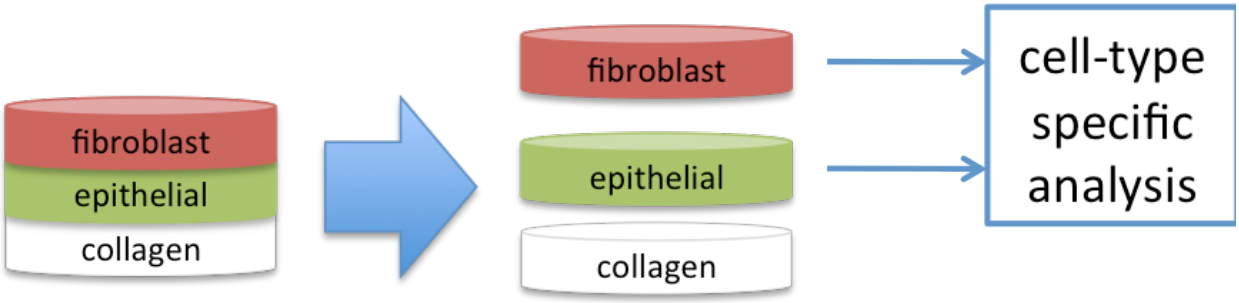

Figure 3.7: Layered 3D sample

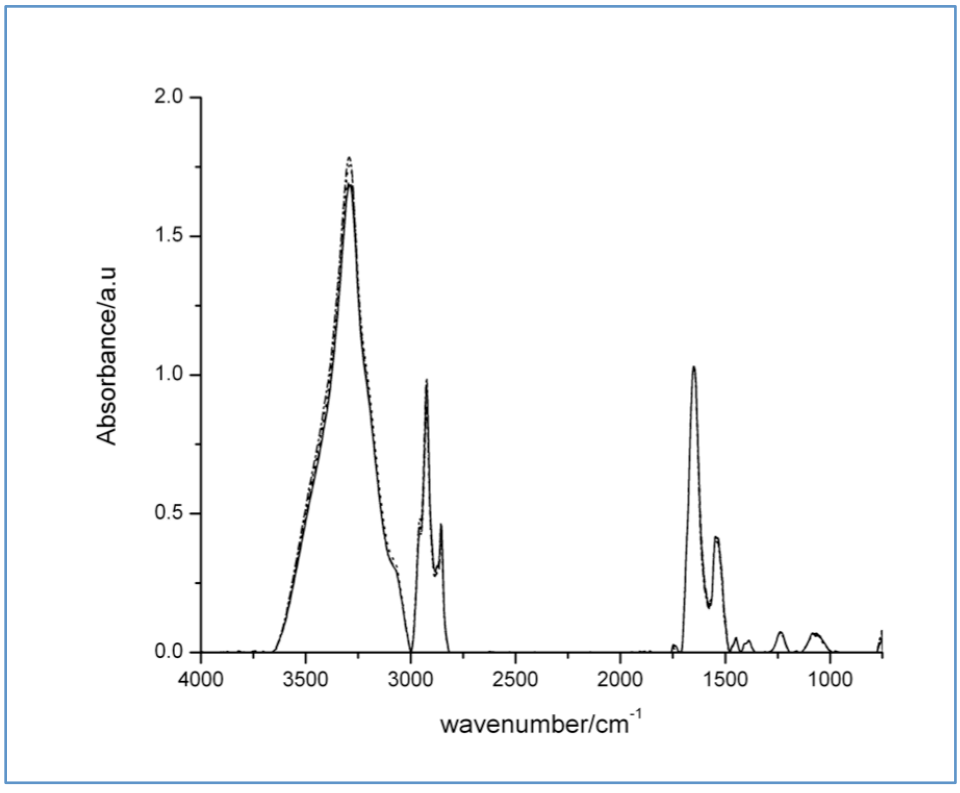

Figure 3.8: Changes in spectra across sample

CHAPTER 4: RESULTS AND DISCUSSION

Section 4.1: Comparison of FT-IR and α-SMA expression using transwell co-culture

For each set of experiments, samples were prepared in duplicate and the experiment was replicated independently in order to show reproducibility of both biological results and chemical spectra.

The transwell co-culture setup (**Figure 3.5**) allows for molecular crosstalk between epithelial cells and fibroblasts and has been extensively used in the literature for this type of experiment (Chu, 2009) (Sadlonova, 2009) (Härmä, 2010). By using this setup, the cells freely diffuse small molecules into the medium continuously, in contrast to using medium conditioned by previous growth with one cell type. For spectral analysis, it is important to keep the cell types separate, as different cell lines have vastly different chemistries (Baker, 2010). The transwell co-culture system is very useful for comparing known biological phenomena with IR signatures, because any IR (or Raman) substrate can be used in the bottom portion of the culture dish. In this experiment, MirrIR Low-E IR reflective slides were cut into pieces, and sterilized before being used. Immunofluorescence staining was also done with the MirrIR slides, and there were no detrimental optical effects of the coated glass surface. Using the MirrIR slides for both immunofluorescence and FT-IR measurements ensured that there was no substrate-specific force felt by the fibroblasts, which could induce α-SMA expression independent of soluble growth factors.

First, the transwell co-culture system was used in order to determine if co-culturing normal primary fibroblasts with tumorigenic breast epithelial cells could result in an activated phenotype, characterized by the expression of α-SMA. This activated phenotype

had been shown previously in fibroblasts isolated from stroma surrounding a tumor *in vivo* (Rønnov-Jessen, 1996). The growth factor TGFβ1 is also known to induce this transformation both *in vitro* and *in vivo* (Rønnov-Jessen, 1995). Co-culture with MCF-7 induced transformation in primary dermal fibroblasts within 6 hours to the same extent as treatment with 1.5 ng/mL TGFβ1 (**Figure 4.1**). In contrast, co-culture with MCF10A, a nontumorigenic breast epithelial cell line, did not result in the expression of α-SMA. The experiment was repeated over a time course of 24 hours, with timepoints being taken at 0 (no co-culture), 6, 12, and 24 hours in order to see if there is an evolution of this phenotypic change over time. From immunofluorescence results, there was no visible change in the amount of α-SMA expression over time (**Figure 4.1**). Rather, the expression was either classified as present or absent.

The same experiment was used in order to prepare samples for analysis using FT-IR spectroscopic imaging. It was hypothesized that looking at the chemical spectra might yield more information about the process of fibroblast activation than antibody-based techniques because of the holistic nature of IR spectra. Changes were seen in the biomolecular fingerprint region (1660-950 cm^{-1}) (**Figure 4.2a**) and also in the C-H stretch region (3000-2875 cm^{-1}) (**Figure 4.3**). In the fingerprint region, changes were primarily seen in peaks at 1080 cm^{-1} and 1224 cm^{-1} (**Figure 4.2b**). These are the asymmetric and symmetric vibrational modes of the phosphate bond, indicative of changes in nucleic acids. There is an increase in the 1080 cm^{-1} peak, which is usually associated with the symmetric phosphate stretching of DNA. These spectra are averaged to cell density, and the cells were serum-starved before the experiment began, and so there should have been little cellular proliferation over the 24 hour time course. The increases seen in the 1080 cm^{-1} peak could

indicate that the cells have become transformed genetically, resulting in aneuploid cells. Aneuploid cells have gone genetically haywire, which is indicated in cancerous phenotypes.

In the C-H stretch region, changes were seen in peaks at 2850 cm^{-1}, 2930 cm^{-1}, and 2960 cm^{-1}. This region of the spectrum is correlated with proteins and also the carbonyl chains of fatty acids (Menendez, 2007). With increasing lengths of time after TGFβ1 stimulation, there was a gradual increase in peak height across all peaks in this region (**Figure 4.4**). In contrast, co-culture with MCF-7 cells yielded a fibroblast response that was more digital, with a very quick increase in peak height at 1080 cm^{-1} after just 6 hours in comparison with the 0h, no co-culture data (**Figure 4.5**). Although there is complete overlap with immunofluorescence results between TGFβ1 stimulation and co-culture with MCF-7 cells, there are some differences in the chemical spectra, which is useful for a more in-depth biochemical analysis of this phenomenon.

Section 4.2 Comparison of FT-IR and Immunofluorescence for 3D co-culture

These experiments were also repeated in a three-dimensional cell culture analog of the transwell culture model. Primary dermal fibroblasts, MCF10A, and MCF-7 cells were embedded in a loose type I collagen hydrogel matrix. Each cell type comprised a single layer of a multilayered culture system (**Figure 3.7**). The layers were prepared separately, which allowed for cells to be cultured together and then separated into layers for single cell type analysis. For this analysis, the fibroblast layer was paraffin embedded and sectioned for FT-IR imaging. For immunofluorescence staining, an antibody specific for α-SMA was used to probe for the presence of myofibroblasts in the bulk of the collagen layer. Confocal microscopy was used in order to determine the presence or absence of the α-SMA protein,

indicating whether or not these cells were activated (**Figure 4B**). The immunofluorescence results remained consistent with the transwell co-culture results, with MCF-7 cells activating fibroblasts along the same time course as TGFβ1 activation. One of the benefits of using a three-dimensional cell culture model is that it is an intermediate between traditional cell culture and human tissue. Cells are known to express surface receptors more faithfully in three-dimensional culture and are also more likely to differentiate in response to external stimuli, for example mesenchymal stem cells are highly sensitive to the elastic modulus of their culture environment (Tibbitt, 2009) (Nelson, 2009). Another use for three-dimensional cell culture in this setup is that the collagen peaks (1283 cm^{-1}, 1236 cm^{-1}, and 1204 cm^{-1}) can be used. These peaks are diagnostically useful when looking at whole tissue sections (Walsh, *in submission*), and there is evidence which shows that changes in collagen spectra can be detected within a certain distance from a tumor (Kong, 2010), which is clinically relevant for cancer pathology. Protein, collagen, and nucleic acid spectra after co-culture with MCF-7 cells in this three-dimensional culture model is shown in **Figure 4.6**. There is an overall increase in the absorption of the collagen peaks after co-culture with MCF-7 cells over time. This could be the result of fibroblasts depositing higher amounts of collagen after receiving cancerous stimuli from the epithelium. The other possibility is that upon fibroblast activation, the stiffening of the cells themselves results in the contraction of the surrounding gel, making local regions appear more collagen-dense in the chemical spectra. As shown in **Figure 4.6**, there is an increase in the nucleic acid peak at 1080 cm^{-1} initially, however after 24 hours this peak has diminished. The 'ebb and flow' of this nucleic acid signature could mean that the chemical signals from MCF-7 have diffused completely throughout the gel after 24 hours, and new simulation is required to

induce gene activation and product formation. A longer time-scale would be needed in order to see if this is the case. This is consistent with changes seen in the transwell co-culture. There is no change in transcription (1224 cm^{-1}) seen in this model compared with the transwell-culture model because the cells are unable to spread out fully within the collagen matrix and thus the cytoplasm is much smaller compared with the nucleus of the cells.

Similarly, peaks in the C-H stretch region are used in this analysis for the three-dimensional cell cultures (**Figure 4.7**). These peaks correlate with both changes in protein conformation and lipid synthesis (Kong, 2010) (Harvey, 2009). From this model, the increase in these peaks over time upon co-culture with MCF-7 cells could be either from changes in the phospholipid membrane or protein synthesis after fibroblast activation. Either explanation is plausible considering the physiologic changes that occur during the fibroblast to myofibroblast phenotypic change.

Section 4.3 FT-IR imaging results from human tumor specimens

In tandem with these cell culture experiments, breast tissue microarrays (TMAs) were purchased (US Biomax, Inc) and cut onto a barium fluoride substrate which allows infrared radiation to pass through the sample without reflecting. Adjacent sections of the same TMA were cut onto normal glass slides for immunohistochemical staining of a panel of diagnostic stains, including vimentin and α-SMA. Vimentin will stain for fibroblasts and other mesoderm-derived tissues. In **Figure 4.8**, the vimentin (in brown) is primarily seen in the stroma between glands. In contrast, α-SMA is a protein found in myofibroblasts and smooth muscle cells which surround blood vessels. **Figure 4.9** shows that only fibroblasts

nearest the cancerous epithelium express α-SMA. This is a cancer-associated signature and is diagnostically relevant.

FT-IR imaging was used in conjunction with IHC staining to mark out unique cell types in order to build a cell classifier (Walsh, *in submission*). This work only looks at the fibroblast and myofibroblast classes, which were developed by looking at the entire TMA. The average cell spectra are shown in **Figure 4.10**. The average absorbance of the myofibroblast class is somewhat decreased compared with the three-dimensional cell culture results. This could be due to absorbance of the collagen matrix surrounding the cells. For the three-dimensional culture results, spectra of individual cells were not picked out from the surrounding matrix, as was done using the artificial classifier. However, the collagen peaks (1300-1050 cm^{-1}), are consistent in shape between the three-dimensional culture model and the tissue sample. This lends credence to using this model as an intermediate between traditional cell culture techniques and real tissue studies.

Section 4.4 Use of ATR FT-IR to show dynamic chemical changes within fibroblasts

Originally, all spectra were collected in the transflection imaging mode (Holton, *in submission*). Average spectra across both confluent and subconfluent areas of the slide were collected. From the transflection measurements, the largest change in chemical spectra across time and sample type was in the two regions pertaining to nucleic acids, 1080 cm^{-1} (asymmetric phosphate) and 1224 cm^{-1} (symmetric phosphate) (Holton, *in submission*). Although α-SMA expression was simply characterized as 'on' in the TGF-β1 treated and MCF-7 co-cultured samples and 'off' in the 0h no co-culture and MCF10A co-cultured samples, IR data showed an evolution of peak height increases over time in the

treatment groups (Holton*, in submission*). Although some discrimination could be made between the nuclear region and that of the cytoplasm, point spectra obtained from 'cytoplasmic' regions were noisy (**Figure 4.11**).

In light of the IR spectra obtained from the measurements obtained in transflection, some samples were scanned using the ATR FT-IR mode in order to increase spatial resolution. This allowed for each fibroblast to be divided into hundreds of pixels with discernible nuclear and cytoplasmic regions (**Figures 4.11-12**). Several hundred pixels from each region were marked as ROIs, averaged and plotted (**Figure 4.12**), resulting in noise reduction (because more pure pixels could be averaged) and higher differences in the spectra between intracellular regions. This allows for a 'subcellular' analysis of the biochemical changes occurring across the sample. In particular, a distinction was made between the nucleus and cytoplasm of the fibroblasts in each sample.

Next, α-SMA expression determined through immunofluorescence was compared directly with ATR FT-IR images (**Figures 4.13-14**). Absorption peaks at 1544 cm^{-1}, 1656 cm^{-1}, and 2932 cm^{-1} gave the highest contrast for stress fibers. These are bands which are related to protein conformational changes and thus are the ones used in this particular analysis. There was no single band which fully described the stress fibers, and so a collection of bands ('chemical signature') was used. Actin isoforms, including α-SMA, are characterized by an acetylated NH_2-terminal decapeptide (Skalli, 1986). However, there are only subtle differences between the isoforms (as little as a 4 amino acid residue change), and thus the spectral data probably cannot discriminate between endogenously expressed F-actin and the stimulated α-SMA. However, global changes in biochemistry in these so-called 'activated fibroblasts' can be distinguished by looking at changes across the spectra.

Finally, using average spectra obtained from marked pixels, an evolution of the chemical changes occurring in NDF over time across all conditions was determined. Although increases in nucleic acids (1080 cm^{-1} and 1224 cm^{-1}) were previously thought to have a nuclear origin (Holton, *in submission*), average spectra obtained from ATR FT-IR measurements show greater increases in the cytoplasm pixels and in particular the 1080 cm^{-1} peak (**Figure 4.15**). This phenotypic change is the result of chemical factors present in the cytoplasm, and it is not necessarily under nuclear control after 24 hours. This makes sense because the fibroblast to myofibroblast transformation is characterized by the expression of a cytoplasmic protein. Protein fiber bundles form and allow the cell to spread out, stiffening the surrounding tissue.

Similarly, in the C-H stretch region (3000 – 2750 cm^{-1}), drastic changes in the cytoplasm under the 24h MCF-7 co-culture condition are seen (**Figure 4.16**). In comparison with the 0h control, the peaks at 2392 cm^{-1} and 2856 cm^{-1} in the 24h MCF-7 co-culture sample were greatly increased while there was a decrease in the peak heights of the 24h TGF-β1 treated sample. This shows that co-culture with MCF-7 likely induces this phenotype much more drastically than stimulation with TGF-β1. MCF-7 cells, having a cancerous phenotype, likely bombard the NDF with chemical signals. Some of these signals may have synergistic effects in regulating the myofibroblast differentiation, which results in an increased response compared with induction of the phenotype by using one growth factor. In addition, this could indicate *de novo* fatty acid production in fibroblasts which are located near cancerous epithelium undergoing this phenotypic change whereas TGF-β1 stimulated cells are simply metabolizing these fatty acids. *De novo* synthesis of fatty acids catalyzed by fatty acid synthase is one of the hallmarks of cancerous epithelium (Harvey,

2009). Fatty acid synthase (FAS) converts acetyl-CoA into malonyl-CoA and its final product is palmityl-CoA, a fatty acid with a 16 carbon chain (Menendez, 2007). The lengthening of this carbon chain is possibly shown by these increases in symmetric and asymmetric CH_2 stretching bands at 2392 cm^{-1} and 2856 cm^{-1}.

Section 4.5 FIGURES

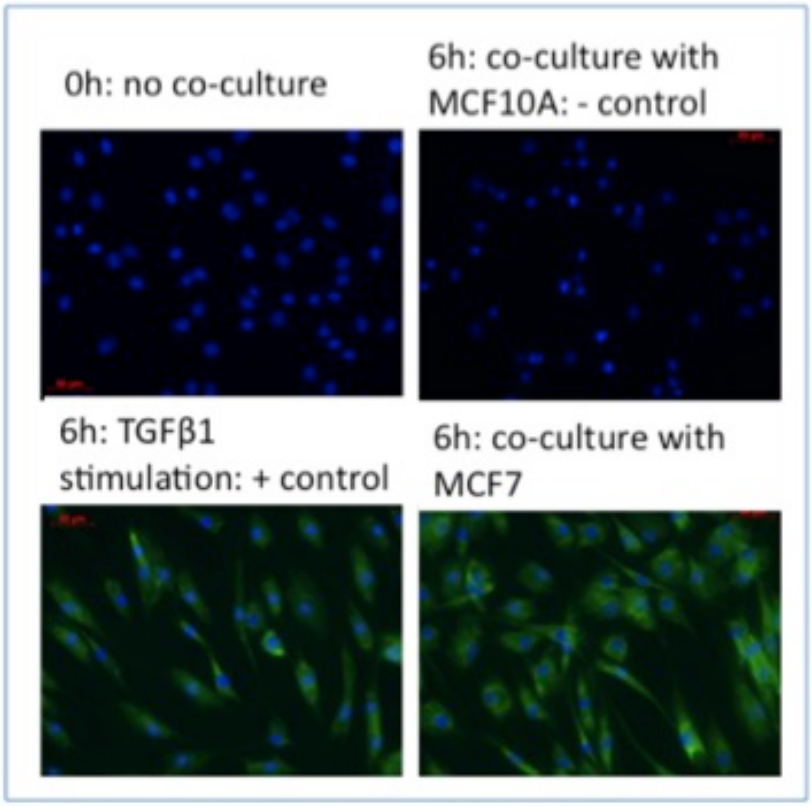

Figure 4.1: Immunofluorescence results

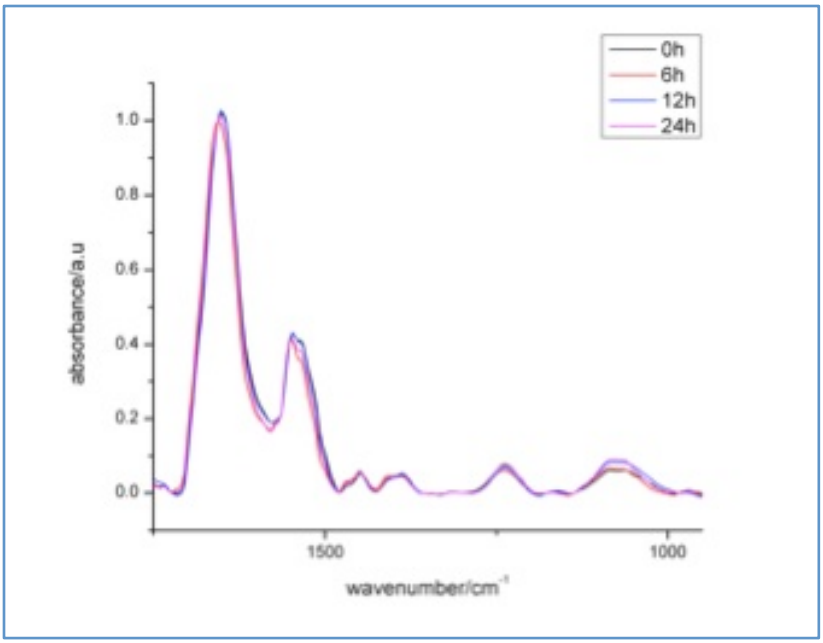

Figure 4.2a: Spectra in biomolecular fingerprint region

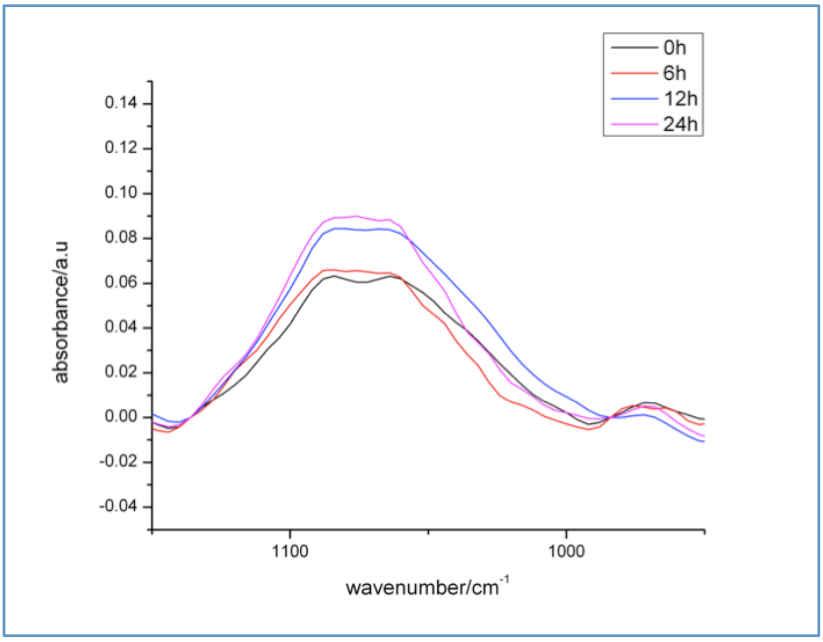

Figure 4.2b: Zoomed in on 1224 cm^{-1} and 1080 cm^{-1}

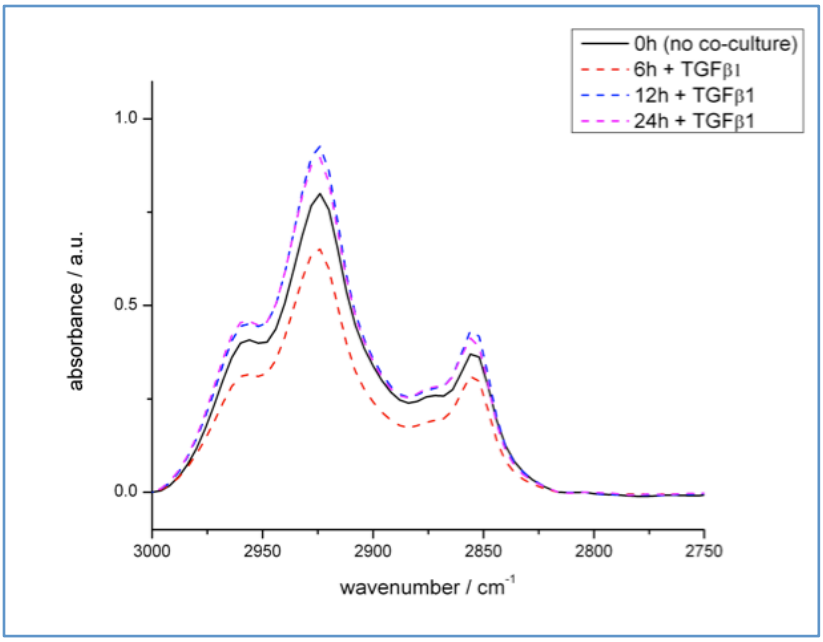

Figure 4.3: C-H stretch region

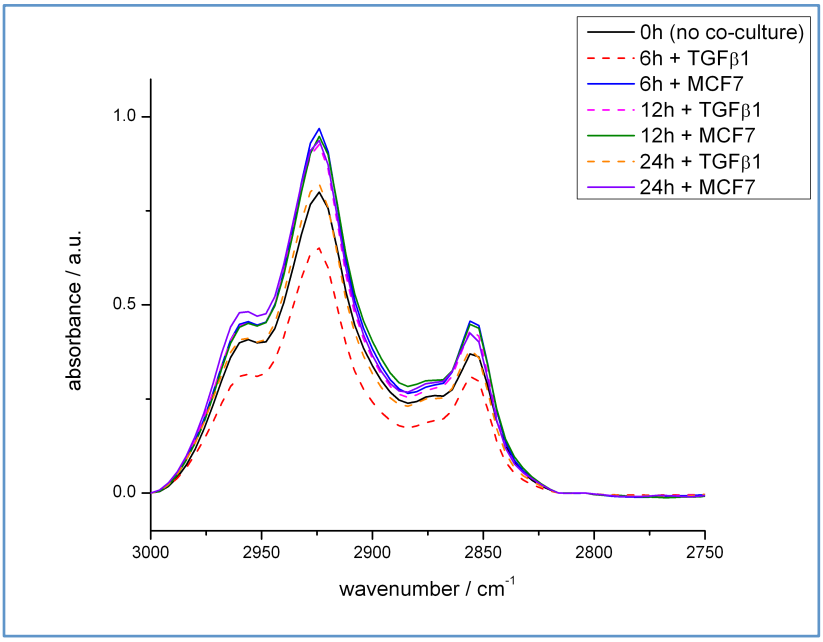

Figure 4.4: Chemical evolution across C-H stretch region

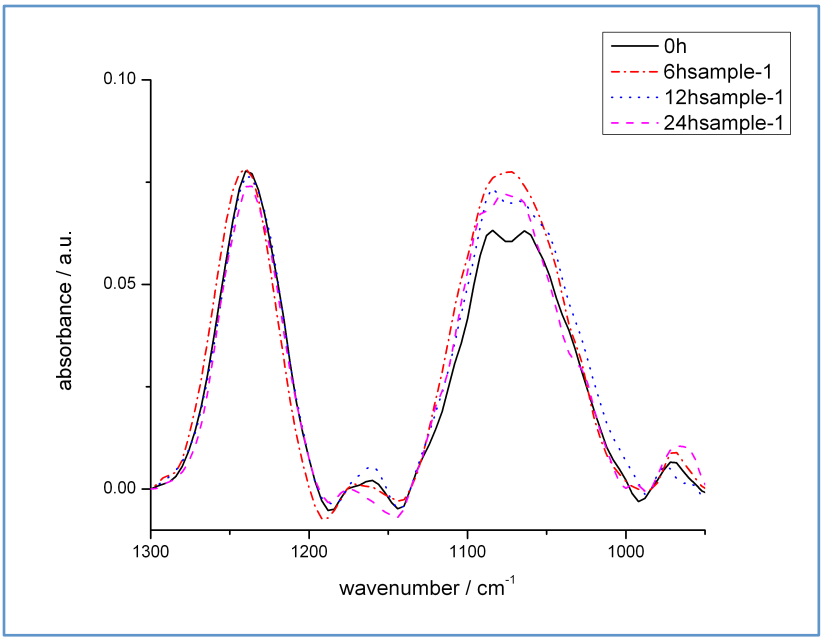

Figure 4.5: Peaks associated with nucleic acids

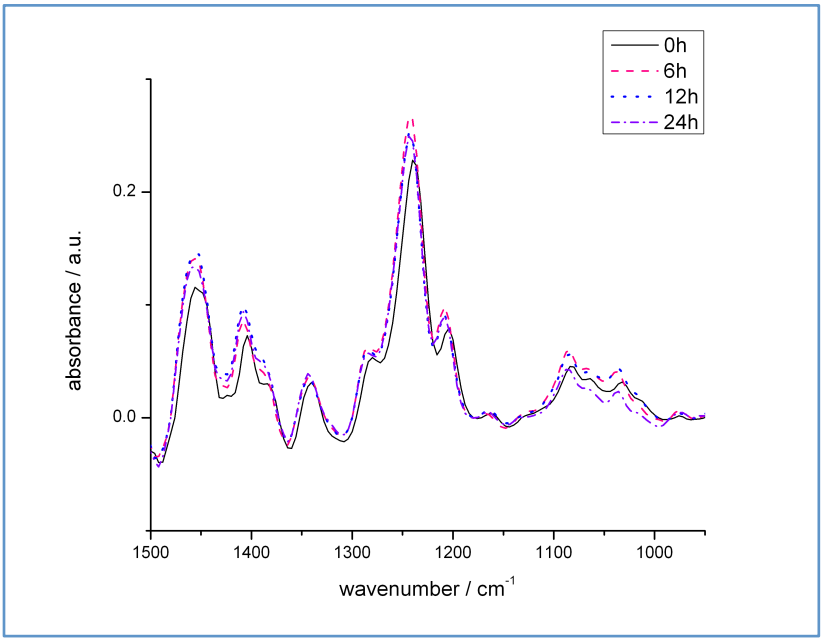

Figure 4.6: Comparison of spectra in 3D co-culture samples

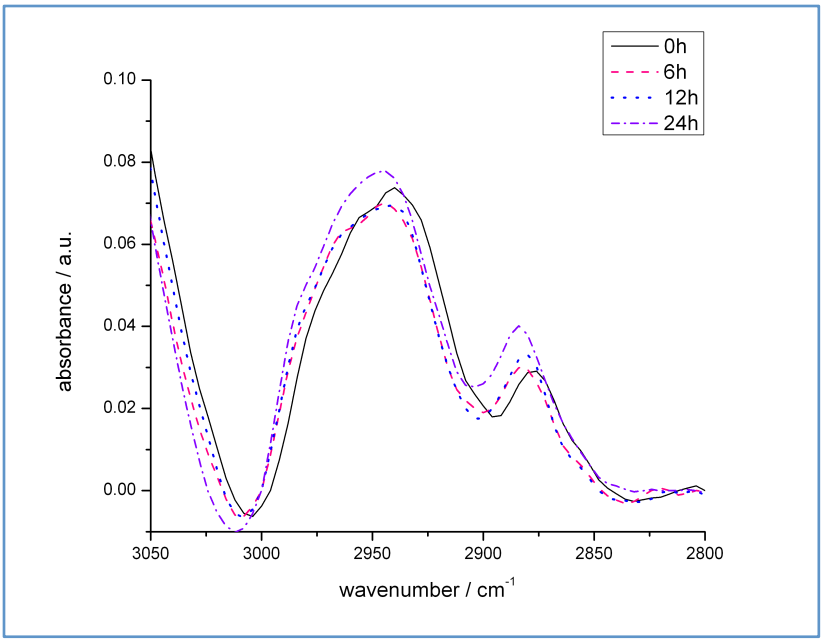

Figure 4.7: C-H stretch region of 3D co-cultures

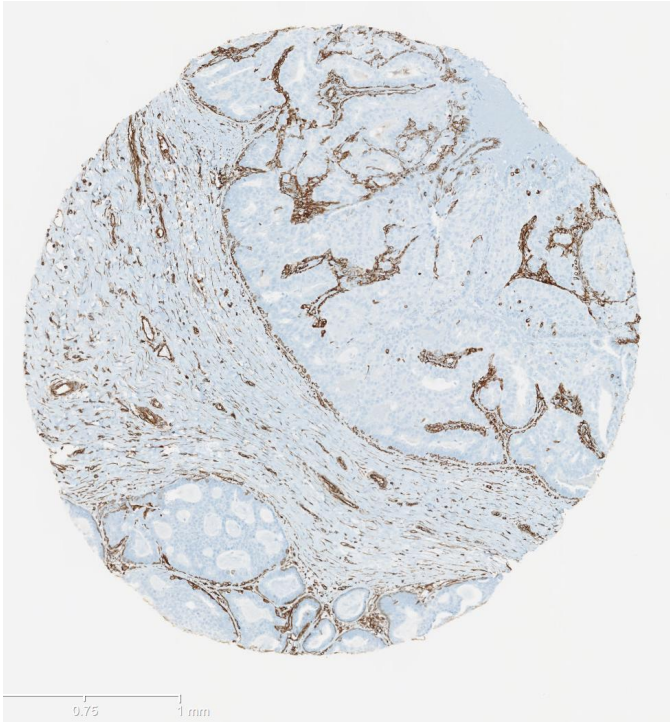

Figure 4.8: Immunohistochemistry: vimentin

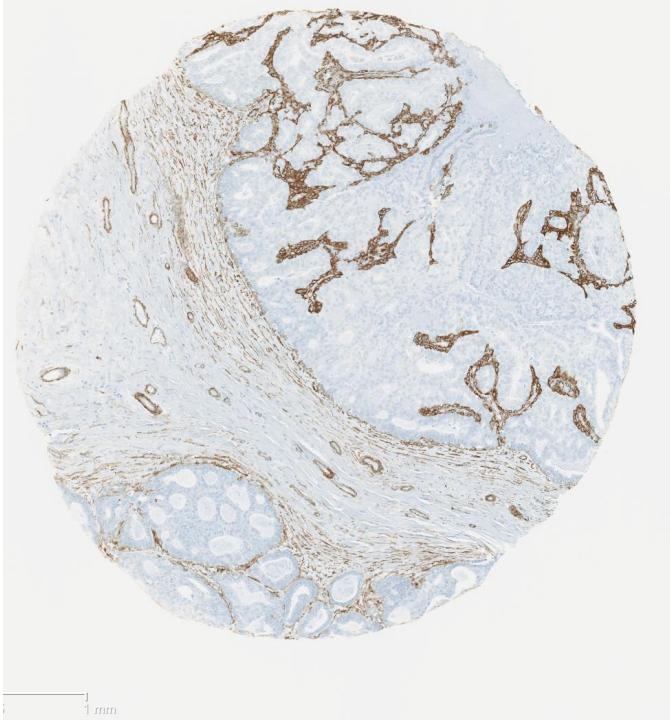

Figure 4.9: Immunohistochemistry: α-SMA

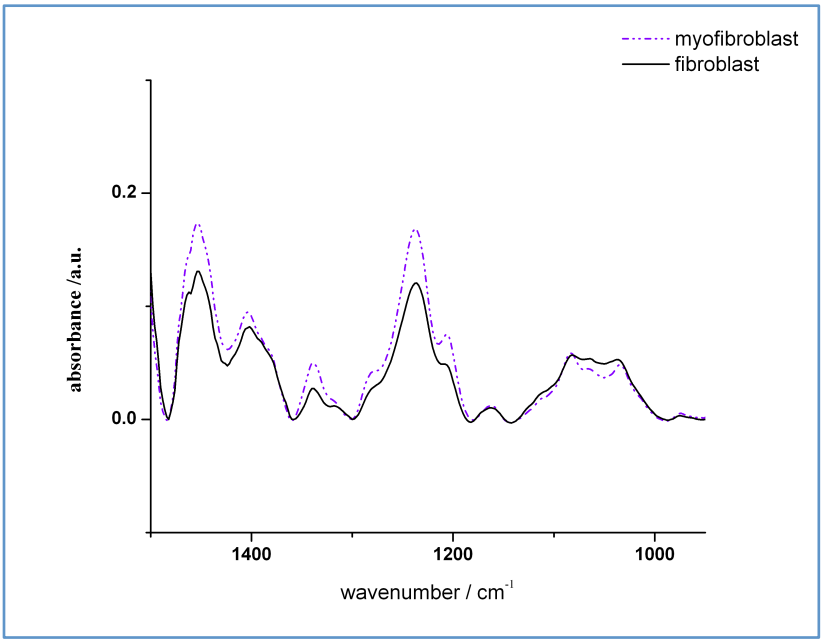

Figure 4.10: Spectra of cell types from TMAs

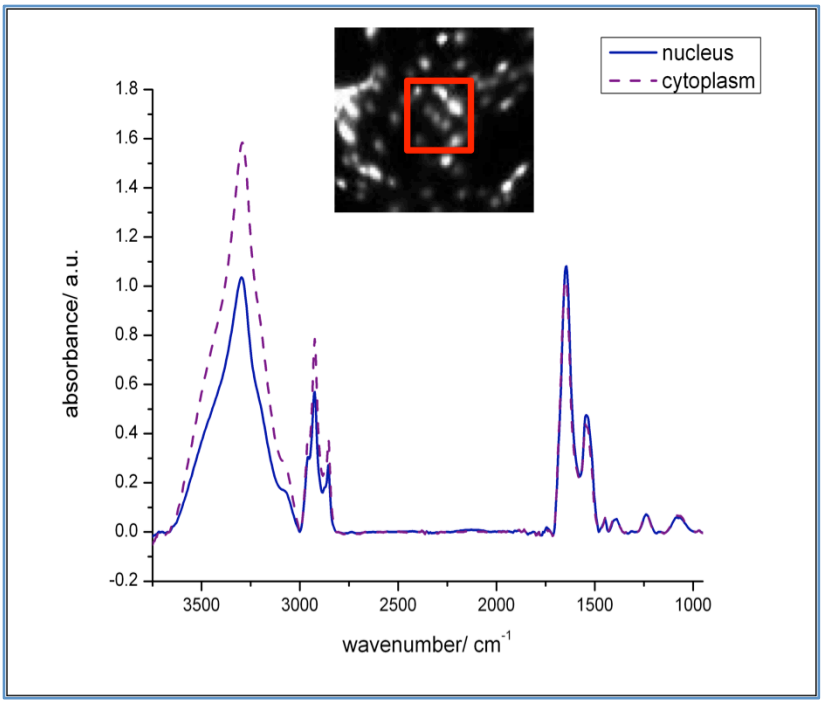

Figure 4.11: Transflection comparison between nucleus and cytoplasm

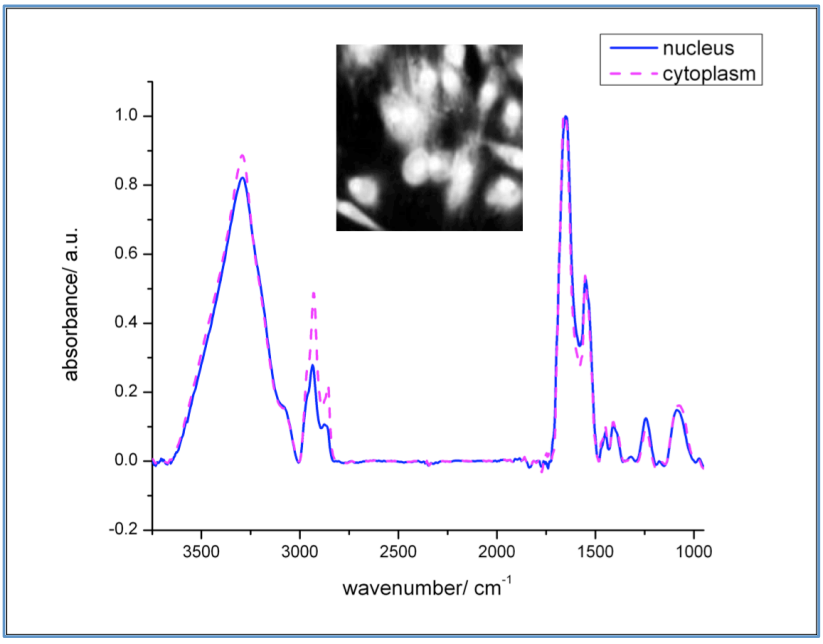

Figure 4.12: ATR comparison between nucleus and cytoplasm

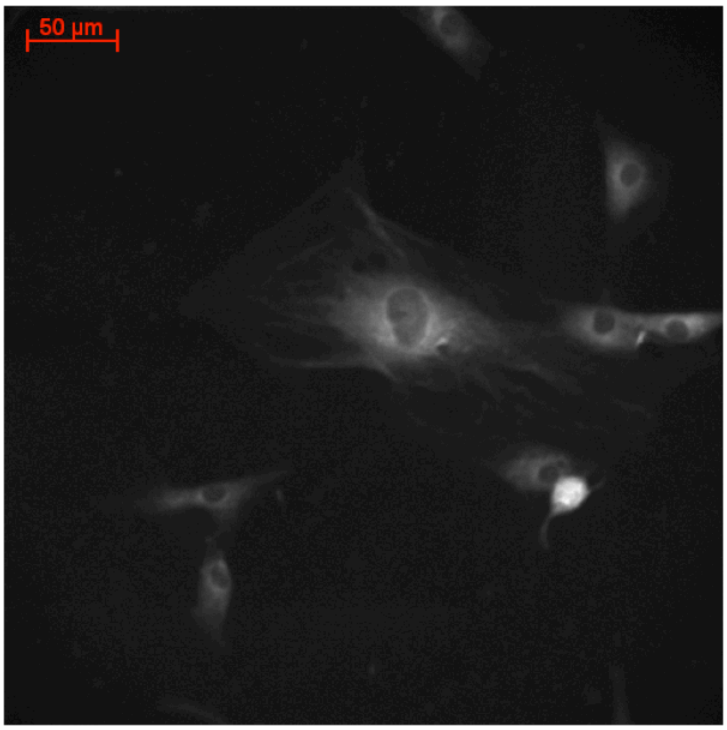

Figure 4.13: α-SMA expression shown using immunofluorescence

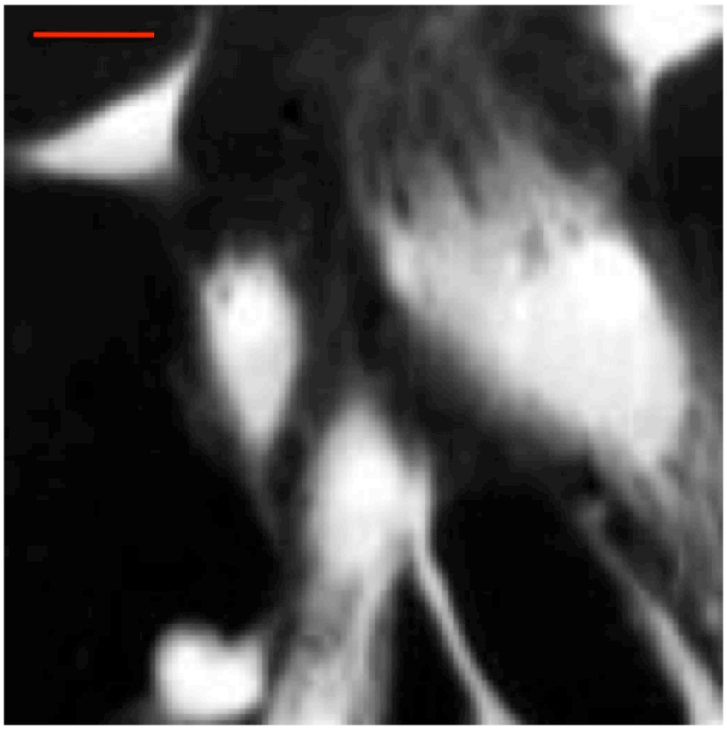

Figure 4.14: ATR image of the band at 1656 cm^{-1} (Amide I)

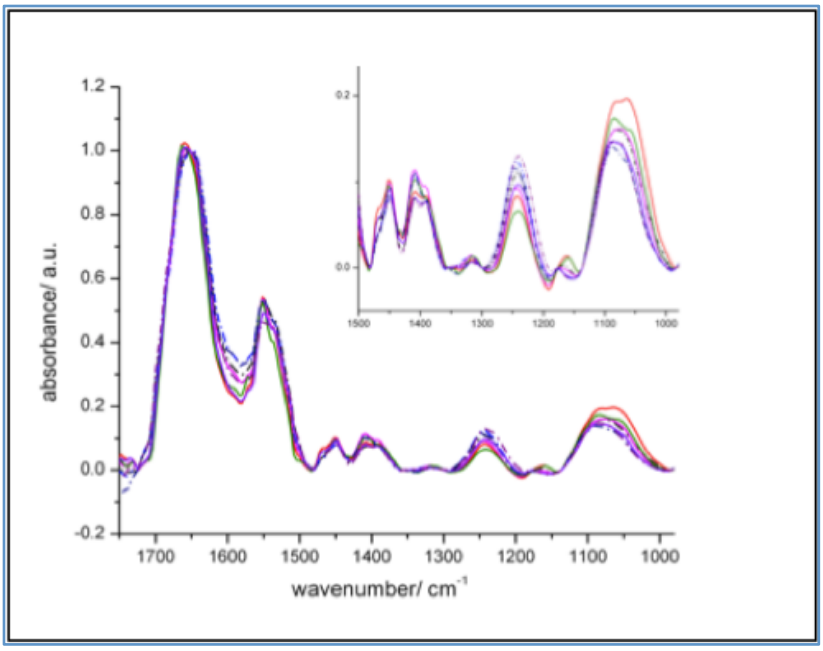

Figure 4.15: Comparison of nucleus and cytoplasm spectra in the biomolecular fingerprint region

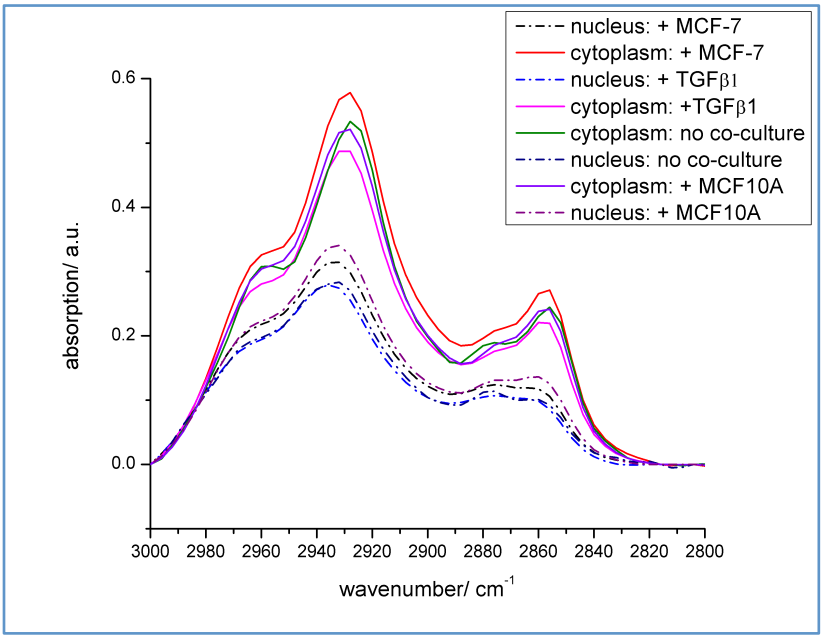

Figure 4.16: Comparison of nucleus and cytoplasm spectra in C-H stretch region

CHAPTER 5: CONCLUSIONS

The presence of an activated stroma surrounding a tumor is characterized by the expression of a single protein, α-SMA. It is advantageous to study cellular phenotypic changes on a more holistic level in order to find potential therapeutic targets that may sequester confined tumors in the stroma, suppressing any further progression. One of the ways to study global biochemical changes between samples is Fourier transform infrared (FT-IR) imaging. Normal adult human primary dermal fibroblasts were cultured on IR-reflective slides so that average chemical spectra could be directly correlated with the expression of α-SMA using immunofluorescence techniques. A three-dimensional culture analog was developed by embedding cells within a type I collagen hydrogel in order to see how the chemical spectra changed compared with the transwell co-culture model. Changes were seen predominantly in the C-H stretch region (3290 cm^{-1}) and phosphate bonds associated with nucleic acids (1224 cm^{-1} and 1080 cm^{-1}). Finally, these cell co-culture models were compared with fibroblasts and myofibroblasts found in whole tumor biopsies from patients diagnosed with breast cancer. By directly comparing the known biological phenomenon of fibroblast activation with the label-free FT-IR imaging, biological assays to determine cancerous phenotypes can be analyzed in a high-throughput manner. Eliminating antibody-based techniques from the workflow reduces variability, time, and costs.

Also, this work describes using ATR FT-IR spectroscopy as a way to further investigate the fibroblast to myofibroblast phenotypic change because its higher spatial resolution allows the visualization of subcellular compartments. By marking pure pixels

and taking average spectra of nuclear and cytoplasmic regions, it was found that this transition is largely due to biochemical changes occurring in the cytoplasm rather than the nucleus. By directly comparing this change to the regular biological technique of immunofluorescent staining for the biomarker α-SMA, a direct comparison was made between biological phenomena and chemical spectra. ATR FT-IR is a powerful technique for understanding global changes in cell biology in order to see which assays to choose next. For example, the evolution in the C-H stretch region of fibroblasts co-cultured with cancerous breast epithelial cells suggests that fatty acid metabolism should be further investigated. Using ATR FT-IR to understand the fibroblast to myofibroblast phenotypic change may have implications in the study of lung fibrosis, wound management, and cancer progression as a diagnostic tool.

REFERENCES

Akselrod, G., Timp, W., Mirsaidov, U., Zhao, Q., & Li, C. "Laser-guided assembly of heterotypic three-dimensional living cell microarrays". *Biophysical journal*, (2006) **91**: 3465-3473.

Albrecht, D., Underhill, G., & Wassermann, T. "Probing the role of multicellular organization in three-dimensional microenvironments". *Nature methods*, (2006) **3**(5): 369-375.

Allinen, M., Beroukhim, R., Cai, L., Brennan, C.,..., & Polyak, K. "Molecular characterization of the tumor microenvironment in breast cancer". *Cancer Cell*, (2004) **6**: 17-32.

Atula, S., Grenman, R., & Syrjänen, S. "Fibroblasts Can Modulate the Phenotype of Malignant Epithelial Cells *in Vitro*". *Experimental cell research*, (1997) **235**:180-187.

Baker, M., Clarke, C., Démoulin, D., & Nicholson, J. "An investigation of the RWPE prostate derived family of cell lines using FT-IR spectroscopy". *The Analyst*, (2010) **135**: 887-894.

Barcellos-Hoff, M., & Medina, D. "New highlights on stroma-epithelial interactions in breast cancer". *Breast Cancer Research*, (2004) **7**(1): 33-36.

Barclay, W., Woodruff, R., Hall, M., & Cramer, S. "A system for studying epithelial-stromal interactions reveals distinct inductive abilities of stromal cells from benign prostatic hyperplasia and prostate cancer". *Endocrinology*, (2005) **146**: 13-18.

Bhowmick, N., Neilson, E., & Moses, H. "Stromal fibroblasts in cancer initiation and progression". *Nature*, (2004), **432**: 332-337.

Bierie, B., & Moses, H. "TGF-[beta] and cancer". *Cytokine & growth factor reviews*, (2006) **17**: 29-40.

Bird, Miljkovic, M., Chernenko, T., Romeo, M., & Diem, M. "Infrared and Raman Microscopy in Cell Biology". *Methods in cell biology*, (2008) **89**: 275-308.

Bissell, M. "Modelling molecular mechanisms of breast cancer and invasion: lessons from the normal gland". *Biochem Soc Trans*, (2007) **35**(Pt 1): 18-22.

Bissell, M., Rizki, A., & Mian, I. "Tissue architecture: the ultimate regulator of breast epithelial function". *Current opinion in cell biology*, (2003) **15**:753-762.

Bogomolny, E., Argov, S., & Mordechai, S. "Monitoring of viral cancer progression using FT-IR microscopy: A comparative study of intact cells and tissues". *Biochimica et Biophysica Acta*, (2008) **1780**: 1038-1046.

Bogomolny, E., Huleihel, M., & Suproun, Y. "Early spectral changes of cellular malignant transformation using Fourier transform infrared microspectroscopy". *Journal of Biomedical Optics*, (2007) **12**(2): 024003-1-9.

Brown, M., Clarke, N., Nicholson, J., & Gardner, P. "Optical artefacts in transflection mode FT-IR microspectroscopic images of single cells on a biological support: the effect of back-scattering into collection optics". *The Analyst*, (2007) **132**: 750-755.

Butcher, D., Alliston, T., & Weaver, V. "A tense situation: forcing tumour progression". *Nature Reviews Cancer*, (2009) **9**:108-122.

Chang, H., Sneddon, J., & Alizadeh, A. "Gene expression signature of fibroblast serum response predicts human cancer progression: similarities between tumors and wounds". *PLoS Biology*, (2004) **2**(2): 0206-0214.

Chaponnier, C., Goethals, M., & Janmey, P. "The specific NH2-terminal sequence Ac-EEED of alpha-smooth muscle actin plays a role in polymerization *in vitro* and *in vivo*". *Journal of Cell Biology*, (1995) **130**(4): 887-895.

Chu, J., Yu, S., Hayward, S., & Chan, F. "Development of a three-dimensional culture model of prostatic epithelial cells and its use for the study of epithelial-mesenchymal transition and inhibition of PI3K pathway in prostate cancer. *The Prostate*, (2009) **69**: 428-442.

Cukierman, E. "A visual-quantitative analysis of fibroblastic stromagenesis in breast cancer progression". *Journal of mammary gland biology and neoplasia*, (2004) **9**(4): 311-324.

Cukierman, E., Pankov, R., & Yamada, K. "Cell interactions with three-dimensional matrices". *Current opinion in cell biology*, (2002), **14**: 633-639.

Debnath, J., & Brugge, J. "Modelling glandular epithelial cancers in three-dimensional cultures". *Nature Reviews Cancer*, (2005), **5**: 675-688.

Debnath, J., Muthuswamy, S., & Brugge, J. "Morphogenesis and oncogenesis of MCF-10A mammary epithelial acini grown in three-dimensional basement membrane cultures". *Methods*, (2003), **30**: 256-268.

Dedhar, Briand, P., Lupu, R., & Bissell, M. "Reciprocal interactions between β1-integrin and epidermal growth factor receptor in three-dimensional basement membrane breast cultures: a different perspective in epithelial biology". *Proc. Natl. Acad. Sci. USA*, (1998) **95**: 14821-14826.

Dhimolea, E., Maffini, M., Soto, A., & Sonnenschein, C. "The role of collagen reorganization on mammary epithelial morphogenesis in a 3D culture model". *Biomaterials*, (2010) **31**: 3622-3630.

Diem, M., Romeo, M., Matthäus, C., & Miljkovic, M. "Comparison of Fourier transform infrared (FT-IR) spectra of individual cells acquired using synchrotron and conventional sources". *Infrared Physics & Technology*, (2004) **45**: 331-338.

Dumas, P., Gazi, E., Brown, M., Clarke, N., & Gardner, P. "Reflection contributions to the dispersion artefact in FT-IR spectra of single biological cells". *The Analyst*, (2009) **134**: 1171-1175.

Erler, J., & Weaver, V. "Three-dimensional context regulation of metastasis". *Clinical and Experimental Metastasis*, (2009) **26**: 35-49.

Even-Ram, S., & Yamada, K. "Cell migration in 3D matrix". *Current opinion in cell biology*, (2005) **17**: 524-532.

Fernandez,D., Bhargava, R., Hewitt, S.M., and Levin, I.W. Infrared spectroscopic imaging for histopathologic recognition. *Nature Biotechnology*, (2005) **23**(4): 469-474.

Fidler, I., Kim, S., & Langley, R. "The role of the organ microenvironment in the biology and therapy of cancer metastasis". *Journal of cellular biochemistry*, (2007) **101**: 927-936.

Finak, G., Bertos, N., Pepin, F., & Sadekova, S. "Stromal gene expression predicts clinical outcome in breast cancer". *Nature medicine*, (2008), **14**(5): 518-527.

Fischbach, C., Chen, R., Matsumoto, T., & Schmelzle, T. "Engineering tumors with 3D scaffolds". *Nature methods*, (2007), **4**(10): 855-860.

Friedl, P. "Dynamic imaging of cancer invasion and metastasis: principles and preclinical applications". *Clinical and Experimental Metastasis*, (2009), **26**: 269-271.

Friedl, P., Zänker, K., & Bröcker, E. "Cell migration strategies in 3-D extracellular matrix: differences in morphology, cell matrix interactions, and integrin function". *Microscopy research and technique*, (1998), **43**: 369-378.

Gazi, E., Dwyer, J., Lockyer, N., Miyan, J., & Gardner, P. "A study of cytokinetic and motile prostate cancer cells using synchrotron-based FT-IR microspectroscopic imaging". *Vibrational Spectroscopy*, (2005), **38**: 193-201.

Goffin, J., Pittet, P., Csucs, G., & Lussi, J. "Focal adhesion size controls tension-dependent recruitment of α-smooth muscle actin to stress fibers". *The Journal of cell biology*, (2006), **172**(2): 259-268.

Grinnell, F. "Fibroblast biology in three-dimensional collagen matrices". *Trends in cell biology*, (2003), **13**(5): 264-269.

Härmä, V., Virtanen, J., & Mäkelä, R. "A comprehensive panel of three-dimensional models for studies of prostate cancer growth, invasion and drug responses". *PLoS One*, (2010) **5**(5): 10431.

Harvey, T., Brown, M., Lockyer, N., & Gardner, P. "A FT-IR microspectroscopic study of the uptake and metabolism of isotopically labelled fatty acids by metastatic prostate cancer". *Vibrational Spectroscopy*, (2009) **50**: 99-105.

Hoffman, R. "Three-dimensional histoculture: origins and applications in cancer research". *Cancer Cells*, (1991) **3**(3): 86-92.

Holton, S. E., Walsh, M. J., & Bhargava, R. (2010). Comparison of fibroblast activation by FT-IR imaging and a-SMA expression. *In Submission* .

Hynes, N., & Watson, C. "Mammary Gland Growth Factors: Roles in Normal Development and in Cancer". *Cold Spring Harb Perspect Biol*, (2010), **2**: a003186.

Ingber, D. "Can cancer be reversed by engineering the tumor microenvironment?" *Seminars in cancer biology*, (2008), **18**: 356-364.

Ippolito, S., Goldberg, B.B., & Ünlü, M.S. "Theoretical analysis of numerical aperture increasing lens microscopy". *Journal of Applied Physics*, (2005), **97**: 053105.

Joyce, J., & Pollard, J. "Microenvironmental regulation of metastasis". *Nature Reviews Cancer*, (2009), **9**: 239-252.

Kalluri, R., & Zeisberg, M. "Fibroblasts in cancer". *Nature Reviews Cancer*, (2006), **6**: 392-401.

Kazarian, S. “New opportunities in micro-and macro-attenuated total reflection infrared spectroscopic imaging: spatial resolution and sampling versatility”. *Applied spectroscopy*, (2003), **57**(4): 381-389.

Kenny, P., & Bissell, M. “Tumor reversion: correction of malignant behavior by microenvironmental cues”. *International Journal of Cancer*, (2003), **107**: 688-695.

Kenny, P., Lee, G., Myers, C., & Neve, R. “The morphologies of breast cancer cell lines in three-dimensional assays correlate with their profiles of gene expression”. *Molecular Oncology*, (2007), **1**(1): 84-96.

Kim, J., Stein, R., & O'Hare, M. “Three-dimensional *in vitro* tissue culture models of breast cancer—a review”. *Breast cancer research and treatment*, (2004), **85**: 281-291.

Kong, R., Reddy, R., & Bhargava, R. “Characterization of tumor progression in engineered tissue using infrared spectroscopic imaging”. *The Analyst*, (2010), **135**: 1569-1578.

Krause, S., Maffini, M., & Soto, A. “A novel 3D in vitro culture model to study stromal-epithelial interactions in the mammary gland”. *Tissue Engineering: Part C*, (2008), **14**(3): 261-271.

Lasch, P., Haensch, W., Naumann, D., & Diem, M. “Imaging of colorectal adenocarcinoma using FT-IR microspectroscopy and cluster analysis”. *Biochimica et Biophysica Acta*, (2004), **1688**: 176-186.

Lasch, P., Pacifico, A., & Diem, M. “Spatially resolved IR microspectroscopy of single cells”. *Biopolymers*, (2002), **67**: 335-338.

Lee, G., Kenny, P., Lee, E., & Bissell, M. “Three-dimensional culture models of normal and malignant breast epithelial cells”. *Nature methods*, (2007), **4**(4): 359-365.

Lee, S., Yoon, K., Jang, S., Ganbold, E., & Uuriintuya, D. “Infrared spectroscopy characterization of normal and lung cancer cells originated from epithelium”. *J. Vet. Sci*, (2009), **10**(4): 299-304.

Lelievre, S., Bissell, M. “The Use of a Human Breast Tumor Progression Series and a 3-D Culture Model to Determine if Nuclear Structure Could Provide a Molecular and Therapeutic Marker”. *J Mammary Gland Biol Neoplasia*, (2010), **15**: 49-63.

Liotta, L., & Kohn, E. “The microenvironment of the tumour–host interface”. *Nature*, (2001), **411**: 375-379.

Liotta, L., & Stetler-Stevenson, W. “Tumor invasion and metastasis: an imbalance of positive and negative regulation”. *Cancer research*, (1991), **51**: 5054s-5059s.

Liu, H., Radisky, D., & Wang, F. “Polarity and proliferation are controlled by distinct signaling pathways downstream of PI3-kinase in breast epithelial tumor cells”. *The Journal of Cell Biology*, (2004), **164**(4): 603-612.

Lutolf, M., & Hubbell, J. “Synthetic biomaterials as instructive extracellular microenvironments for morphogenesis in tissue engineering”. *Nature biotechnology*, (2005), **23**(1): 47-55.

Maffini, M., Calabro, J., Soto, A., & Sonnenschein, C. “Stromal regulation of neoplastic development: age-dependent normalization of neoplastic mammary cells by mammary stroma”. *The American journal of pathology ,* **167**(5), 1405-10.

Martin, K., Patrick, D., Bissell, M., & Fournier, M. “Prognostic breast cancer signature identified from 3D culture model accurately predicts clinical outcome across independent datasets”. *PLoS One*, (2008), **3**(8): e2994.

McDaniel, S., Rumer, K., Biroc, S., & Metz, R. “Remodeling of the mammary microenvironment after lactation promotes breast tumor cell metastasis”. *American Journal of Pathology*, (2006), **168**(2): 608-620.

Meade, A., Lyng, F., Knief, P., & Byrne, H. “Growth substrate induced functional changes elucidated by FT-IR and Raman spectroscopy in in–vitro cultured human keratinocytes”. *Analytical and Bioanalytical Chemistry*, (2007), **387**: 1717-1728.

Menendez, J., & Lupu, R. “Fatty acid synthase and the lipogenic phenotype in cancer pathogenesis”. *Nature Reviews Cancer*, (2007), **7**: 763-777.

Moses, H., & Barcellos-Hoff, M. “TGF-{beta} Biology in Mammary Development and Breast Cancer”. *Cold Spring Harb Perspect Biol* doi: 10.1101/cshperspect.a003277.

Mourant, J., Short, K., & Carpenter, S. “Biochemical differences in tumorigenic and nontumorigenic cells measured by Raman and infrared spectroscopy”. *Journal of Biomedical Optics*, (2005), **10**(3): 031106.

Mourant, J., Yamada, Y., & Carpenter, S. “FTIR spectroscopy demonstrates biochemical differences in mammalian cell cultures at different growth stages”. *Biophysical journal*, (2003), **85**: 1938-1947.

Mueller, M., & Fusenig, N. “Friends or foes—bipolar effects of the tumour stroma in cancer”. *Nature Reviews Cancer*, (2004), **4**: 839-849.

Muschler, J., & Streuli, C. “Cell-Matrix Interactions in Mammary Gland Development and Breast Cancer”. *Cold Spring Harb Perspect Biol*, (2010) 2:a003202.

Nehls, V., & Drenckhahn, D. “Heterogeneity of microvascular pericytes for smooth muscle type alpha-actin”. *The Journal of cell biology*, (1991), **113**(1): 147-154.

Nelson, C., & Bissell, M. “Modeling dynamic reciprocity: engineering three-dimensional culture models of breast architecture, function, and neoplastic transformation”. *Seminars in cancer biology*, (2005), **15**: 342-352.

Nelson, C., & Tien, J. “Microstructured extracellular matrices in tissue engineering and development”. *Current opinion in biotechnology*, (2006), **17**: 518-523.

Nelson, C., Khauv, D., & Bissell, M. “Change in cell shape is required for matrix metalloproteinase-induced epithelial-mesenchymal transition of mammary epithelial cells”. *Journal of cellular biochemistry*, (2008), **105**: 25-33.

Nelson, W. “Remodeling epithelial cell organization: Transitions between Front–Rear and Apical–Basal polarity”. *Cold Spring Harbor Perspectives in Biology*, (2009), 1:a000513.

Olumi, A., Grossfeld, G., Hayward, S., & Carroll, P. "Carcinoma-associated fibroblasts direct tumor progression of initiated human prostatic epithelium". *Cancer research*, (1999), **59**: 5002-5011.

Ong, V., Carulli, M., Xu, S., Khan, K., & Lindahl, G. "Cross-talk between MCP-3 and TGF [beta] promotes fibroblast collagen biosynthesis". *Experimental Cell Research*, (2009), **315**: 151-161.

Östman, A., & Augsten, M. "Cancer-associated fibroblasts and tumor growth-bystanders turning into key players". *Current Opinion in Genetics & Development*, (2009), **19**: 67-73.

Pampaloni, F., Reynaud, E., & Stelzer, E. "The third dimension bridges the gap between cell culture and live tissue". *Nature Reviews: Molecular Cell Biology*, (2007), **8**: 839-845.

Pizzo, A., Kokini, K., & Vaughn, L. "Extracellular matrix (ECM) microstructural composition regulates local cell-ECM biomechanics and fundamental fibroblast behavior: a multidimensional perspective". *Journal of Applied Physiology*, (2005), **98**: 1909-1921.

Polyak, K., & Kalluri, R. "The Role of the Microenvironment in Mammary Gland Development and Cancer". *Cold Spring Harbor Perspectives in Biology*, (2010), doi:10.1101/cshperspect.a003244.

Prestwich, G. "Simplifying the extracellular matrix for 3-D cell culture and tissue engineering: a pragmatic approach". *Journal of cellular biochemistry*, (2007), **101**: 1370-1383.

Provenzano, P., Eliceiri, K., & Campbell, J. "Collagen reorganization at the tumor-stromal interface facilitates local invasion". *BMC Medicine*, (2006), **4**: 38-54.

Rønnov-Jessen, L. "Stromal reaction to invasive cancer: the cellular origin of the myofibroblast and implications for tumor development". *The Breast Journal,* (1996), **2**(5): 320-339.

Rønnov-Jessen, L., & Petersen, O. "The origin of the myofibroblast in breast cancer. Recapitulation of tumor environment in culture unravels diversity and implicates converted fibroblasts and recruited smooth muscle cells". *Journal of Clinical Investigation*, (1995), **95**: 859-873.

Ramesh, J., Salman, A., Hammody, Z., & Cohen, B. "FTIR microscopic studies on normal and H-Ras oncogene transfected cultured mouse fibroblasts". *European Biophysics Journal*, (2001), **30**: 250-255.

Richter, C., Reinhardt, M., Giselbrecht, S., ..., & Welle, A. "Spatially controlled cell adhesion on three-dimensional substrates". *Biomedical Microdevices*, (2010), **12**: 787-795.

Romeo, Mohlenhoff, B., Jennings, M., & Diem, M. "Infrared micro-spectroscopic studies of epithelial cells". *Biochimica et Biophysica Acta*, (2006), **1758**: 915-922.

Roskelley, C., & Bissell, M. "The dominance of the microenvironment in breast and ovarian cancer". *Seminars in cancer biology*, (2002), **12**: 97-104.

Rozenchan, P., & Carraro, D. "Reciprocal changes in gene expression profiles of cocultured breast epithelial cells and primary fibroblasts". *International Journal of Cancer*, (2009), **125**: 2767-2777.

Sadlonova, A., Bowe, D., Novak, Z., ..., & Frost, A.R. “Identification of molecular distinctions between normal breast-associated fibroblasts and breast cancer-associated fibroblasts”. *Cancer Microenvironment*, (2009), **2**: 9-21.

Salk, J., Fox, E., & Loeb, L. “Mutational heterogeneity in human cancers: origin and consequences.” *Ann. Rev. Pathol. Mech. Dis.*, (2010), **5**: 51-75.

Salman, A., Sahu, R., Bernshtain, E., & Zelig, U. “Probing cell proliferation in the human colon using vibrational spectroscopy: a novel use of FTIR-microspectroscopy”. *Vibrational Spectroscopy*, (2004), **34**: 301-308.

Schmeichel, K., & Bissell, M. “Modeling tissue-specific signaling and organ function in three dimensions”. *Journal of Cell Science*, (2003), **116**: 2377-2388.

Schmeichel, K., Weaver, V., & Bissell, M. “Structural cues from the tissue microenvironment are essential determinants of the human mammary epithelial cell phenotype”. *Journal of mammary gland biology and neoplasia*, (1998), **3**(2): 201-213.

Schwartz, M., Fairbanks, B., Rogers, R., Rangarajan, R., Zaman, M., & Anseth, K. “A synthetic strategy for mimicking the extracellular matrix provides new insight about tumor cell migration:. *Integrative Biology ,* (2010), **2**: 32-40.

Shekhar, M., & Pauley, R. “Host microenvironment in breast cancer development: extracellular matrix–stromal cell contribution to neoplastic phenotype of epithelial cells in the breast”. *Breast Cancer Research*, (2003), **5**(3): 130-135.

Skalli, O., Ropraz, P., & Trzeciak, A. “A monoclonal antibody against alpha-smooth muscle actin: a new probe for smooth muscle differentiation”. *The Journal of cell biology*, (1986), **103**(6-2): 2787-2796.

Skobe, M., & Fusenig, N. “Tumorigenic conversion of immortal human keratinocytes through stromal cell activation”. *Proceedings of the National Academy of Sciences USA*, (1998), **95**: 1050-1055.

Sommer, A., Tisinger, L., & Marcott…, C. “Attenuated total internal reflection infrared mapping microspectroscopy using an imaging microscope”. *Applied Spectroscopy*, (2001), **55**(3): 252-256.

Sorrell, J., & Caplan, A. “Fibroblast heterogeneity: more than skin deep”. *Journal of Cell Science*, (2004), **117**: 667-675.

Stuelten, C., Busch, J., Tang, B., Flanders, K., Oshima, A., Sutton, E., et al. “Transient tumor-fibroblast interactions increase tumor cell malignancy by a TGF-Beta mediated mechanism in a mouse xenograft model of breast cancer”. *PloS one ,* (2010), **5**(3): e9832.

Sung, S., & Chung, L. “Prostate tumor-stroma interaction: molecular mechanisms and opportunities for therapeutic targeting”. *Differentiation*, (2002), **70**: 506-521.

Tibbitt, M., & Anseth, K. “Hydrogels as extracellular matrix mimics for 3D cell culture”. *Biotechnology and bioengineering*, (2009), **103**(4): 655-663.

Tlsty, T., & Coussens, L. “Tumor stroma and regulation of cancer development”. *Annu. Rev. Pathol. Mech. Dis.*, (2006), **1**: 119-50.

Tlsty, T., & Hein, P. “Know thy neighbor: stromal cells can contribute oncogenic signals”. *Current Opinion in Genetics & Development*, (2001), **11**: 54-59.

Trier, S., Eliceiri, K., Keely, P., Friedl, A., & Beebe, D. “Control of 3-dimensional collagen matrix polymerization for reproducible human mammary fibroblast cell culture in microfluidic devices”. *Biomaterials*, (2009), **30**: 4833-4841.

Underwood, J., & Nickerson, J.A. “The ultrastructure of MCF-10A acini”. *Journal of cellular physiology*, (2006), **208**: 141-148.

Ünlü, M.S., Ippolito, S. B., Eraslan, M.G., Thorne, S., Vamivakas, A., ..., & Leblebici, Y. “High Resolution Backside Imaging and Thermography using a Numerical Aperture Increasing Lens”. *Technical Proceedings of the 2004 NSTI Nanotechnology Conference and Trade Show*, (2004), **3**: 8-10.

Walsh, M., Bruce, S., Pant, K., Carmichael, P., & Martin, F.L. “Discrimination of a transformation phenotype in Syrian golden hamster embryo (SHE) cells using ATR-FT-IR spectroscopy”. *Toxicology*, (2009), **258**: 33-38.

Walsh, M., Mayerich, D., & Bhargava, R. “Stainless Staining”. *In Submission*. (2010).

Wang, X., Sun, L., Maffini, M., Soto, A., & Sonnenschein, C. “A complex 3D human tissue culture system based on mammary stromal cells and silk scaffolds for modeling breast morphogenesis and function”. *Biomaterials*, (2010), **31**: 3920-3929.

Weaver, V., Petersen, O., & Wang, F. “Reversion of the malignant phenotype of human breast cells in three-dimensional culture and in vivo by integrin blocking antibodies”. *The Journal of cell biology*, (1997), **137**(1): 231-244.

Weigelt, B., Peterse, J.L., & van’t Veer, L.J. “Breast cancer metastasis: markers and models”. *Nature Reviews Cancer*, (2005), **5**: 591-602.

Wiseman, B., & Werb, Z. “Stromal effects on mammary gland development and breast cancer”. *Science*, (2002), **296**: 1046-1049.

Wolf, K., Alexander, S., Schacht, V., ..., & Friedl, P. “Collagen-based cell migration models in vitro and in vivo”. *Seminars in cell & developmental biology*, (2009), **20**: 931-941.

Wood, B., Quinn, M., Tait, B., Ashdown, M., Hislop, T., Romeo, M., & McNaughton, D. “FTIR microspectroscopic study of cell types and potential confounding variables in screening for cervical malignancies”. *Biospectroscopy ,* (1998), **4**: 75-91.

Yalcin-Ozuysal, Ö., & Brisken, C. “From normal cell types to malignant phenotypes”. *Breast Cancer Research*, (2009), **11**(6): 306-308.

Yamada, K., & Cukierman, E. “Modeling tissue morphogenesis and cancer in 3D”. *Cell*, (2007), **130**: 601-610.

Yilmaz, M., Christofori, G., & Lehembre, F. “Distinct mechanisms of tumor invasion and metastasis”. *Trends in molecular medicine*, (2007), **13**(12): 535-541.